



CAA PAPER 99008

**LIGHTNING STRIKES TO  
HELICOPTERS OVER THE  
NORTH SEA**

CIVIL AVIATION AUTHORITY, LONDON

Price £26.00

CAA PAPER 99008

**LIGHTNING STRIKES TO  
HELICOPTERS OVER THE  
NORTH SEA**

CIVIL AVIATION AUTHORITY, LONDON, DECEMBER 1999

© Civil Aviation Authority 1999

ISBN 0 86039 763 7

Printed and distributed by  
Westward documedia Limited, 37 Windsor Street, Cheltenham, England

## Foreword

Following the accident to an Aerospatiale AS332L Super Puma in January 1995, which resulted from a lightning strike to the carbon composite tail rotor blades, it was suggested that the lightning strike threat in the North Sea is more severe than might be expected in most other parts of the world. A precise understanding of this threat level was required in order to ensure that the protection afforded by the current design requirements is adequate under all operating conditions likely to be incurred by UK registered aircraft.

AEA Technology were awarded a contract to investigate the lightning threat to helicopters operating in the North Sea. EA Technology and the Met. Office also participated in the study. They were also tasked with assessing whether the meteorological conditions prevailing at the time of the strike were significant to the probability of a strike occurring.

Assessments were made of the variation in Strike Polarity Distribution for the North Sea and the meteorological conditions determined for strikes to helicopters as reported by the Mandatory Occurrence Reporting system.

This report has been prepared by the Meteorological Office and a further report, CAA Paper 99007, on the study has been prepared by AEA Technology.



## Contents

1	INTRODUCTION	1
2	THE DATA	2
2.1	Synoptic charts	2
2.2	Satellite data	2
2.3	Model data	2
2.4	Sferic data	3
2.5	Radiosonde data	3
3	QUALITATIVE RESULTS	4
3.1	Synoptic charts and satellite imagery	4
3.1.1	30 October 1992 at 10.04: 60.97°N 1.42°E	4
3.1.2	15 January 1993 at 16.00: 57.08°N 00.60°W	5
3.1.3	18 February 1993 at 17.06: 60.17°N 1.2°E	6
3.1.4	20 February 1993 at 11.25: 60.08°N 1.05°W	7
3.1.5	3 October 1994 at 13.50: 60.30°N 00.32°E	8
3.1.6	19th January 1995 at 12.34: 58.47°N 00.85°E	9
3.1.7	21 February 1995 at 09.18: 59.33°N 1.00°E	10
3.1.8	1 March 1995 at 09.07: 60°N 1.00°W	11
3.1.9	8 December 1995 at 10.48: 60.33°N 00.33°E	12
3.1.10	8 February 1996 at 10.30: 60.68°N 1.25°E	13
3.1.11	26 November 1996 at 14.56: 53.85°N 1.42°E	14
3.1.12	Summary	14
3.2	Model data	15
3.2.1	30 October 1992 at 10.04: 60.97°N 1.42°E: 2000 ft	16
3.2.2	15 January 1993 at 16.00: 57.08°N 00.60°W: 2000 ft	17
3.2.3	18 February 1993 at 17.06: 60.17°N 1.2°E: 2000 ft	18
3.2.4	20 February 1993 at 11.25: 60.08°N 1.05°W: 3000 ft	20
3.2.5	3 October 1994 at 13.50: 60.30°N 00.32°E: 1500 ft	22
3.2.6	19 January 1995 at 12.34: 58.47°N 00.85°E: 3000 ft	23
3.2.7	21 February 1995 at 09.18: 59.33°N 1.00°E: 2000 ft	25
3.2.8	1 March 1995 at 09.07: 60°N 1.00°W: 2000 ft	26
3.2.9	8 December 1995 at 10.48: 60.33°N 00.33°E: 2000 ft	28
3.2.10	8 February 1996 at 10.30: 60.68°N 1.25°E: 1500 ft	29
3.2.11	26 November 1996 at 14.56: 53.85°N 1.42°E: 2000 ft	31
3.2.12	Summary	32
4	QUANTITATIVE RESULTS	33
4.1	Sferics	33
4.2	Convective cloud (from synoptic charts)	34
4.3	Convective cloud (from radiosonde ascents)	35

	4.3.1	Convective cloud base, cloud depth, CAPE and helicopter altitude	36
	4.3.2	Acceleration	42
	4.3.3	Slantwise convection	42
5		REGRESSION ANALYSIS	43
	5.1	The independent variables	43
	5.2	The dependent variable	44
	5.3	Results	44
6		DISCUSSION	48
7		SUMMARY	49
8		FUTURE WORK	50
9		REFERENCES	51

## 1 INTRODUCTION

This report presents an investigation into the meteorological conditions associated with lightning strikes to helicopters over the North Sea. Most of these strikes are probably triggered by the presence of the helicopter, since for a significant number of the incidents the crew report no prior lightning activity (Plumer et al. 1996). The investigation thus concentrates on case studies of strike incidents rather than on the general occurrence of lightning.

It was originally intended to examine incidents dating back to 1988. However changes in the acquisition and archiving of meteorological data meant that data would often have been inconsistent amongst incidents. Since many of the changes took place during 1992 it was decided that only incidents occurring after mid-October 1992 would be considered. There were 11 incidents meeting this criterion for which accurate times and locations were available. Ten of these incidents occurred off the coast of Scotland (including the areas around the Orkney and Shetland Islands) and the remaining incident occurred off the coast of England. For convenience these areas will be referred to as Lerwick and Hemsby respectively, being the names of the nearby radiosonde stations.

An important finding of the investigation was that cumulonimbus clouds were present in the North Sea area for all 11 of the incidents, suggesting a relationship between helicopter lightning strikes and convective cloud. The investigation also led to an equation for predicting lightning strike risk. This equation was derived by comparing Numerical Weather Prediction (NWP) data for the incidents with NWP data for some days on which strikes did not occur. The equation could potentially be used to produce forecasts of the lightning strike risk.

The content of the report is as follows. Section 2 describes the meteorological data used in the investigation. Section 3 is a qualitative analysis of the general meteorological conditions surrounding the incidents, and Section 4 is a more quantitative analysis of these conditions concentrating particularly on convective cloud properties. Section 5 contains the comparison between the NWP data for the strike and non-strike cases, and Section 6 is a discussion. Section 7 is a summary of the work and Section 8 contains suggestions for future work.

## 2 THE DATA

Synoptic charts, satellite images, NWP data, sferic data and radiosonde data were all extracted from Met. Office archives for the 11 lightning strike incidents. These data will be referred to as the strike data set. NWP and radiosonde data were also extracted for 24 days when thunderstorms or deep convective clouds were seen by ground observing stations in the Shetlands and along the eastern coast of the UK. These data were for comparison purposes and will be referred to as the null data set. In selecting the null data set it was assumed that helicopter flights took place on the days in question but that no strikes occurred. The Civil Aviation Authority confirmed this assumption.

The null data set consisted of 21 dates in the Lerwick area and 3 dates in the Hemsby area, with the Lerwick dates being in winter and the Hemsby dates being in summer. The incident locations assumed for the Lerwick null cases were all 59°N 1°E, the average location of the Lerwick strike cases. Similarly the locations assumed for the Hemsby null cases were all 53.85°N 1.42°E, the location of the one strike that occurred in the Hemsby area.

### 2.1 Synoptic charts

Three UK observation charts (issued hourly), a Europe analysis chart (issued once every 3 hours) and a North Atlantic analysis chart (issued once every 6 hours) were retrieved for times just prior to each incident. These charts give a good indication of the general synoptic (large-scale) situation. They show cloud type, cloud amount, cloud base, pressure, pressure change, precipitation type, visibility, temperature, dew-point temperature, wind speed, and wind direction. Areas of low and high pressure are plotted, as are fronts and troughs. The charts are not reproduced in this report as they are illegible in A4 format, but they are described in detail in *Section 3.1 Synoptic charts and satellite imagery*.

### 2.2 Satellite data

Satellite images, especially when animated and viewed in sequence, can also give a good indication of the synoptic situation. Images from the geostationary satellite Meteosat were examined. These images have a lower resolution than images from the National Oceanic and Atmospheric Administration (NOAA) polar orbiting satellite, but they cover a larger area and are updated more frequently. Furthermore NOAA images are split over 2 time passes, which can make interpretation of the synoptic situation difficult. Typically 13 images were obtained from Meteosat for each incident, consisting of 5 infrared, 5 visual and 3 water vapour images. These were valid for times just prior to the incident, and example images are shown in *Section 3.1 Synoptic charts and satellite imagery*.

### 2.3 Model data

Model data were obtained from the Limited Area Model (LAM) configuration of the Met. Office Numerical Weather Prediction (NWP) model. The LAM was used in preference to the Global Model and the Mesoscale Model because it offered better resolution than the former and better North Sea coverage than the latter. Furthermore LAM archives were available over a longer period than Mesoscale Model archives and the loss of terrain information contained in the Mesoscale Model was irrelevant because all of the incidents occurred at sea. The LAM has a horizontal resolution of approximately 45 km at North Sea latitudes.

Data on model levels up to 250 hPa (approximately 38,000 feet) were obtained for the analysis time closest to and preceding each incident, where analysis times are every 3 hours from 00 UTC (Universal Time Clock). The model data were wind speed, wind direction, temperature, relative humidity, large scale vertical velocity, dynamic rain rate, convective rain rate, convective cloud base, convective cloud top, cloud liquid water and cloud ice. Cloud liquid water and cloud ice were not available for all analysis times or on the same model levels as other parameters, and were unavailable before 1994. Convective rain rate was also unavailable before 1994.

Data on the model level closest to the altitude of the incident were examined as contour plots. Data were also examined as vertical cross-section plots passing as closely as possible through the incident location. Contour and cross-section plots are presented in *Section 3.2 Model data* for each incident.

#### 2.4 Sferic data

Lightning discharges produce low frequency radio signals called atmospherics or sferics. The Met. Office Arrival Time Difference system detects these signals and calculates the time and location of a lightning discharge from the different times taken for the signals to reach different receivers. Times and locations were retrieved for all of the sferics detected on the day of each strike incident. Their significance is discussed in *Section 4.1 Sferics*.

#### 2.5 Radiosonde data

Radiosondes attached to weather balloons are released at 6 or 12 hour intervals from Met. Office outstations across the UK. They are also released by other National Met. Services. Radiosonde ascents give vertical profiles through the atmosphere of temperature, dew-point temperature, wind speed, and wind direction. Radiosonde data were obtained for Orland, Stavanger, Boulmer, Stornoway, Lerwick and Hemsby and the locations of some of these sites are shown in Figure 1. Inspection of the synoptic charts gave a guide as to which of these sites and which of the ascents at that site would best sample the air mass present at the time and location of each incident. The ascents are examined in detail in *Section 4.3 Radiosonde data*.



Figure 1: Radiosonde sites

### 3 QUALITATIVE RESULTS

#### 3.1 Synoptic charts and satellite imagery

Synoptic charts and satellite images relating to each incident are described here in qualitative terms to establish similarities between the incidents. For each of the case studies the first paragraph describes the synoptic charts and the second paragraph describes the satellite images.

METEOSAT EB 30 OCT 1992 09:00 UTC



**Figure 2: Infrared satellite image at 09 UTC, 30 October 1992**

##### 3.1.1 30 October 1992 at 10.04: 60.97°N 1.42°E

A low-pressure centre of 1000 hPa was centred on 63.3°N 3.2°E. A cold front ran from this centre in a north-east to south-west direction across the Scottish Highlands, meeting the Scottish coast just east of Inverness. It is estimated that the front crossed the incident site at 07 UTC. The incident occurred in a data sparse area but the nearest observers reported cumulonimbus, deep cumulus, stratocumulus, stratus and cirrostratus cloud. Cloud cover varied from 4 to 8 oktas (eighths). Rain, hail and snow showers were also reported. Winds were 5–10 kt at the surface in a north-north-westerly direction.

The satellite imagery shows a large quantity of high fibrous cloud (possibly cumulonimbus anvils) over the east coast of Scotland and the northern North Sea. This cloud was moving eastwards. The incident took place on the northern edge of the cloud where large storms can be seen.



**Figure 3: Infrared satellite image at 16 UTC, 15 January 1993**

3.1.2 *15 January 1993 at 16.00: 57.08°N 00.60°W*

A large low-pressure area with 2 adjacent lows was centred on 64°N 10°W. This area was associated with an occluded front which had a triple point (the place where an occluded front separates into cold and warm fronts) at 61°N 5°E. The low-pressure area had moved from 48°N 23°W in the space of 24 hours. It is estimated that the cold front passed over the incident site at 11 UTC. The surface winds were 25–30 kt in a west-south-westerly direction. Cumulonimbus, deep cumulus and altocumulus clouds were observed, along with snow and sleet showers.

The satellite imagery shows a large area of convective cloud following some way behind the cold front. The clouds are notably much larger than those in the other case studies. The largest and most eastern convective cloud reached the east coast of Scotland at approximately 16 UTC, coinciding with the location and time of the lightning strike incident.

METEOSAT IR 18 FEB 1993 16:00 UTC



**Figure 4: Infrared satellite image at 16 UTC, 18 February 1993**

3.1.3 *18 February 1993 at 17.06: 60.17°N 1.2°E*

At 17 UTC a 978 hPa low-pressure centre at 64.5°N 6°W had an occluded front with a triple point at 65.5°N 5.3°E. The cold front probably passed over the incident site at 10 UTC moving westwards. Winds were reported to be 20–30 kt. Data are sparse in the area surrounding the incident but a few observers reported cumulonimbus and deep cumulus cloud at 7 oktas. Snow and rain showers were also reported.

The visible and infrared satellite images show a large area of convective cloud following behind the cold front. The infrared picture also shows 2 areas of what look like cirrus or cirrostratus cloud (again possibly cumulonimbus anvils) growing and merging to form a second band of cloud following behind the cold front.



**Figure 5: Infrared satellite image at 11 UTC, 20 February 1993**

3.1.4 *20 February 1993 at 11.25: 60.08°N 1.05°W*

A low-pressure centre of 980 hPa located at 67°N 0°E at 09 UTC had an occluded front associated with it, the triple point being at 59°N 4°E. This low-pressure centre moved to 64.5°N 5°E by 11UTC. It is estimated that the warm front passed over the incident site at about 06 UTC and the cold front by about 07 UTC. The winds were south-westerly ahead of the warm front, west-north-westerly between the warm and cold fronts, and north-westerly behind the cold front, where they were typically of strength 30–35 kt. At 11 UTC, stratocumulus, altostratus/nimbostratus, cumulonimbus, dense cirrus and altocumulus were all observed in the vicinity. Slight and moderate rain showers were visible from the north-east coast of Scotland.

The visible satellite imagery shows the frontal cloud in layer form moving south-westwards. The trailing edge of this cloud crossed the incident site at the reported time of the incident. Convective cloud followed on behind the cold front. The layer cloud tops are brighter in the infrared image than the convective cloud tops, indicating that the layer cloud tops were higher.

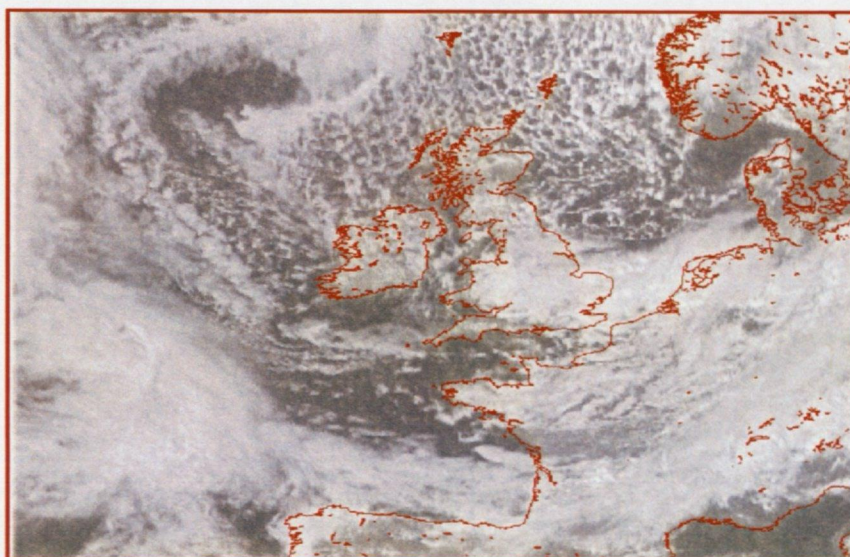


**Figure 6: Visible satellite image at 14 UTC, 3 October 1994**

3.1.5 *3 October 1994 at 13.50: 60.30°N 00.32°E*

A low-pressure centre off the southern coast of Norway had a trough associated with it, which was moving south. The trough moved about 200 miles over the period 11–14 UTC and probably passed over the incident site at about 08 UTC. A large area of convective activity followed the trough southwards. Winds were uniform at about 20 kt at the surface. A high-pressure region of 1025 hPa was located at 58°N 19°W. A second low-pressure region of 980 hPa was located at 60°N 20°W. Clouds observed in the vicinity were deep cumulus, cumulonimbus and stratocumulus. Cloud cover was about 5 oktas. Slight snow and hail showers were reported.

The visible and infrared satellite pictures confirm the large area of convective activity reported on the synoptic charts.

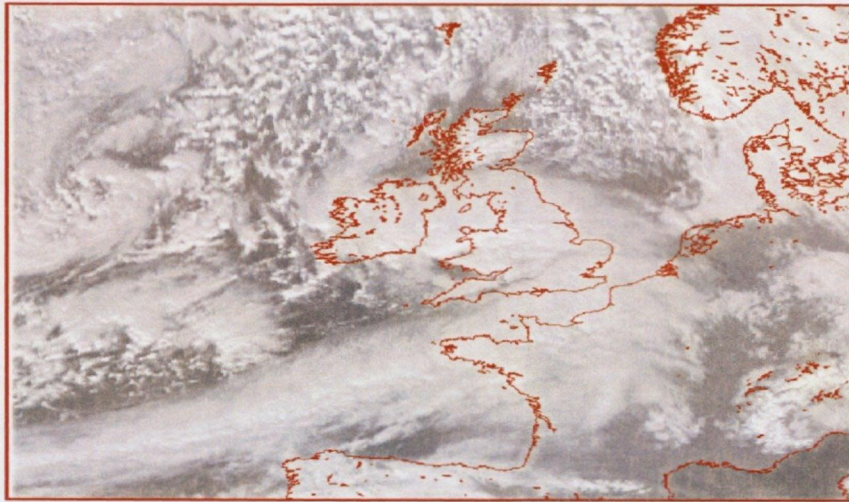


**Figure 7: Visible satellite image at 13 UTC, 19 January 1995**

3.1.6 *19th January 1995 at 12.34: 58.47°N 00.85°E*

There was a low-pressure centre of 970 hPa over the east coast of southern Ireland and another of 956 hPa at 22°W 60.5°N. Together these caused southerly winds of about 25 kt to flow across the North Sea. A cold front was moving westwards over Norway. A surface trough was plotted in a north–south direction across the North Sea with many sferics. This trough is not apparent from surface observations of wind and it is assumed that the forecaster on duty obtained information on the existence of the trough from another source. This source could have been upper-air charts or satellite imagery. It is estimated that the trough was overhead the incident site at 10 UTC. Cumulonimbus, cumulus, stratocumulus and altocumulus clouds were reported at the nearest observation sites. Cloud cover was in the range 4–7 oktas and showers of snow, snow pellets and small hail were present. Slight rain showers were also reported.

Cumulonimbus clouds with anvils were to the north and therefore downwind of the helicopter strike. Deep cumulus and cumulonimbus clouds without anvils were to the south.



**Figure 8: Infrared satellite image at 09 UTC, 21 February 1995**

3.1.7 *21 February 1995 at 09.18: 59.33°N 1.00°E*

A low-pressure region was centred at 55°N 6°E at 06 UTC. It had an associated warm front followed by a cold front. Winds over the North Sea were south-westerly. A second low-pressure centre positioned just to the north of the Outer Hebrides was associated with a trough, which stretched across the western Highlands of Scotland and the Irish Sea to Northern Ireland. The main feature affecting the North Sea was a trough orientated north-west to south-east and moving north-eastwards across the sea. At the time of the lightning strike the trough was approximately overhead. Cumulonimbus, cumulus, altocumulus and cirrus clouds were reported around the incident in the 2–8 okta range, with most observations reporting 5–7 oktas. Moderately heavy rain showers, slight snow showers, showers of snow pellets/small hail and squalls were all observed in the vicinity of the incident at 09 UTC.

The satellite pictures show a swirl of cloud associated with the low-pressure area near the Hebrides. Another large area of predominantly stratiform cloud but also containing cumulonimbus, cumulus and altocumulus cloud, can be seen stretching over the western half of the North Sea to the coast of Norway. The sea is visible as a dark area between these 2 cloud masses. The trough seen on the synoptic charts coincides with this dark area on the satellite picture.

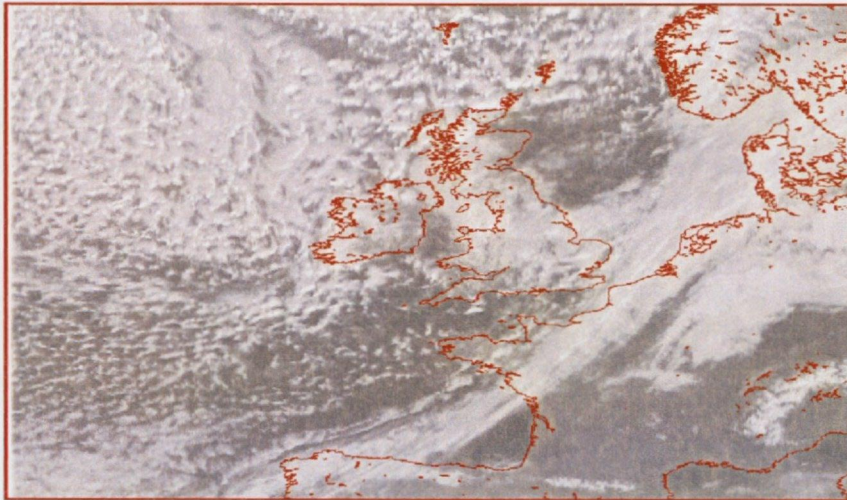


**Figure 9: Visible satellite image at 10 UTC, 1 March 1995**

3.1.8 *1 March 1995 at 09.07: 60°N 1.00°W*

A low-pressure centre of 960 hPa positioned at 68°N 0°E caused moderate westerly winds of approximately 25 kt over the incident site. A large number of observations plotted on the synoptic chart show cumulonimbus clouds over the northern part of the North Sea. An isolated sferic report is shown to the north-east of the incident site at 62°N 2°E. Showers of hail, snow and sleet were observed over the North Sea area. A cold front stretching from northern Spain, through south-east England, and across the North Sea to the northern tip of Denmark probably passed over the incident site in the small hours of the morning.

The large convective clouds plotted on the charts can be seen in both the visible and infrared satellite images.



**Figure 10: Visible satellite image at 11 UTC, 8 December 1995**

3.1.9 *8 December 1995 at 10.48: 60.33°N 00.33°E*

There was a low-pressure centre of 1014 hPa at 58°N 3°W, moving north-westwards. A warm front stretched from this low-pressure centre along the 60°N latitude line, turning south at 10°E to reach down to 45°N 20°E. The winds were south-easterly. A trough was plotted on the 07 UTC chart in a north-west to south-east orientation and stretched from the low centre to 56.5°N 4°E. It is estimated that the trough was over the incident site at the time of the strike. Clouds in the vicinity of the strike at 10 UTC and 11 UTC were cumulus, stratocumulus, altocumulus and cumulonimbus. All observers reported 7–8 oktas of cloud cover. Slight rain showers, intermittent rain and continuous rain were all reported in the vicinity of the strike. An isolated spheric was plotted on the 11 UTC chart just to the east of the incident location.

A visible satellite image was not available until 10 UTC due to the time of year. The 10 UTC and 11 UTC images show fragmented cloud indicative of the convective cloud plotted on the charts. The infrared picture shows this fragmentation less clearly, indicating that the convective cloud was probably not very deep.

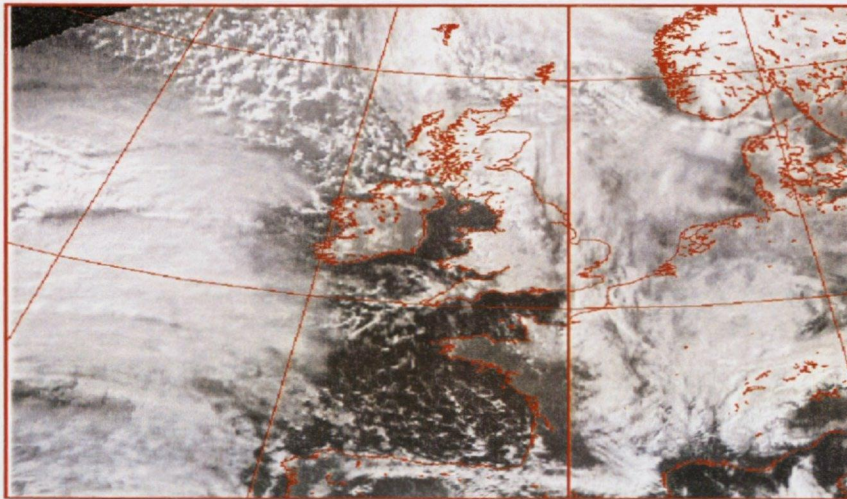


**Figure 11: Visible satellite image at 10 UTC, 8 February 1996**

3.1.10 *8 February 1996 at 10.30: 60.68°N 1.25°E*

A low of approximately 992 hPa was located at 67°N 22°W and was associated with an occluded front. The occlusion curled east and south such that its bottom end was at 59°N 2°W. A second occlusion, also moving eastwards, followed the first with approximately 5° of longitude between them. A second low-pressure centre of 1004 hPa was positioned over Aberdeen and a third occlusion stretched south from there along the eastern coast of the UK. The clouds reported in the vicinity at the time of the incident were stratocumulus, deep cumulus, cumulonimbus and altocumulus. Slight to moderate snow showers were also reported. The wind was southerly at about 20–25 kt.

Infrared satellite images pick out the higher clouds associated with the 3 occlusions and show that the incident occurred between the 2 occlusions to the north of Aberdeen. In this gap 2 layers of cloud are visible, the lower taking on the form of cloud streets and the higher likely to be medium level altocumulus. The 10 UTC visible satellite picture shows 2 convective clouds that are not apparent in the infrared image, indicating that the convection was not very deep. These convective clouds appear to have been over the incident site at the time of the incident.



**Figure 12: Visible satellite image at 14 UTC, 26 November 1996**

3.1.11 *26 November 1996 at 14.56: 53.85°N 1.42°E*

This incident took place some 7° further south than the other incidents. A low-pressure centre of 1000 hPa was at 52°N 9°E, causing north-easterly winds of 10–15 kt to flow across the southern half of the North Sea. A high-pressure centre was located at 62°N 2°W. A second low of 967 hPa was located off the western coast of Scotland and the associated occluded front was moving rapidly eastwards to collide with the south-westwards moving air over the North Sea. Another occluded front associated with this second low was in a north-west to south-east orientation off the south coast of Ireland. Clouds in the vicinity of the strike at 14 and 15 UTC were deep cumulus, stratocumulus, cumulonimbus and altocumulus. Cloud cover was 6–7 oktas to the west and north and generally 3 oktas to the south. Slight rain showers were reported.

Unfortunately the 12 and 15 UTC visible images are missing and by 16 UTC it was dark, but the 13 and 14 UTC images show a large area of convective cloud moving south-westwards between Norway and East Anglia. The occluded front associated with the second area of low-pressure described above is clearly visible approaching from the west.

3.1.12 *Summary*

An obvious similarity between the 11 strike cases is the presence of cumulonimbus clouds. Convective activity was reported in land observations plotted on synoptic charts and confirmed by satellite imagery for every case. Other features of note are that

- In 5 of the cases the helicopter lightning strike followed the passage of a cold front 3–7 hours previously. In another 4 of the cases a trough was either at the

incident location or had passed through the location in the preceding 6 hours. In a further case an occluded front had recently passed through the incident location. For the final case no fronts were in the vicinity.

- Precipitation was present in the vicinity for all 11 cases. In 2 of the cases the precipitation was all frozen (snow or hail), in 3 of the cases it was all non-frozen (rain), and in 6 of the cases it was both frozen and non-frozen.
- Winds varied in strength and direction with no apparent correlations between the cases.

### 3.2 Model data

NWP data for each incident are described in this section by two paragraphs. The first paragraph describes contour plots in the horizontal plane on the model level closest to the helicopter altitude, and the second paragraph describes vertical cross-sections through the incident location taken perpendicular to the wind direction. Vertical cross-sections of wind speed and temperature will only be mentioned if they differed from the typical profile of wind speed increasing and temperature decreasing with altitude. Note that rain rates, cloud ice content and cloud liquid water content were not available for 1992 and 1993, and so are not discussed for incidents occurring in those years.

For each incident a contour plot and a vertical cross-section plot are shown, to illustrate points made in the text. In the contour plots the helicopter position is marked by a black diamond. In the vertical cross-sections the horizontal location of the helicopter is at the centre of the horizontal axis, while the vertical location is marked by an unlabelled tick mark on the vertical axis.

Some useful conversion information is given in Table 1.

Temperature (in Kelvin) = Temperature (in °C) + 273		
Wind speed (in m s <sup>-1</sup> ) ≈ 0.5 × Wind speed (in knots)		
Vertical velocity (in Pa s <sup>-1</sup> ) ≈ 0.1 × Vertical velocity (in m s <sup>-1</sup> ) ≈ 0.3 × Vertical velocity (in ft s <sup>-1</sup> )		
Pressure (hPa)	Height (m)	Height (ft)
1013.2	0	0
1000	111	364
900	988	3,243
800	1949	6,394
700	3012	9,882
600	4206	13,801
500	5574	18,289
400	7185	23,574
300	9164	30,065

**Table 1: Conversion information assuming the International Standard Atmosphere**

3.2.1 30 October 1992 at 10.04: 60.97°N 1.42°E: 2000 ft

The incident location had air temperature in the range 274–275 K, with warmer air to the south and cooler air to the north. Winds were light at 4–8 m s<sup>-1</sup> in a westerly direction. They were northerly to the west and southerly to the east of the incident location. The highest winds were in the range 10–12 m s<sup>-1</sup> both to the east and to the west of the incident. Humidity at the incident location was in the range 80–85% with moister air (>95%) to the east and dryer air (55–60%) to the west. Air was ascending across the whole of the northern North Sea. Convective cloud depth was greatest to the east of the incident, where it was between 500 and 600 hPa deep, as shown in Figure 13.

The humidity profile, Figure 14, shows a region of high humidity at 500 hPa, where it was greater than 95%. A dryer layer was present below this region, with humidity in the range 65–70%, and lower still the air became moister again. The vertical velocity profile shows a small layer of descending air at very high levels to the north-east of the incident but elsewhere air was ascending.

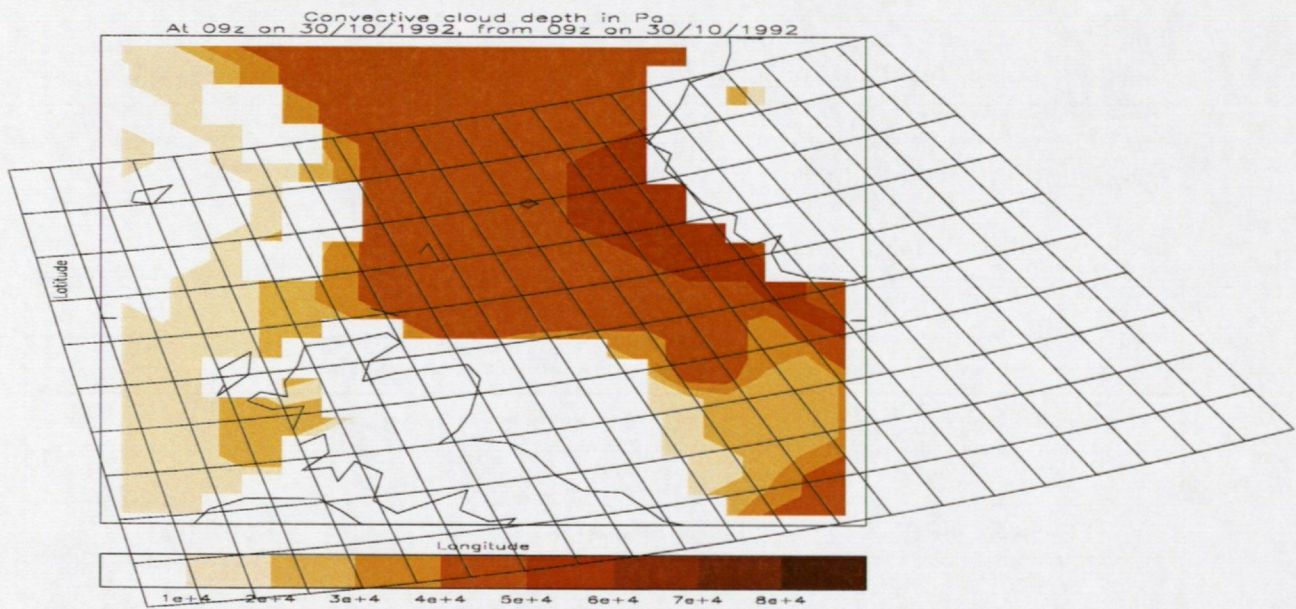
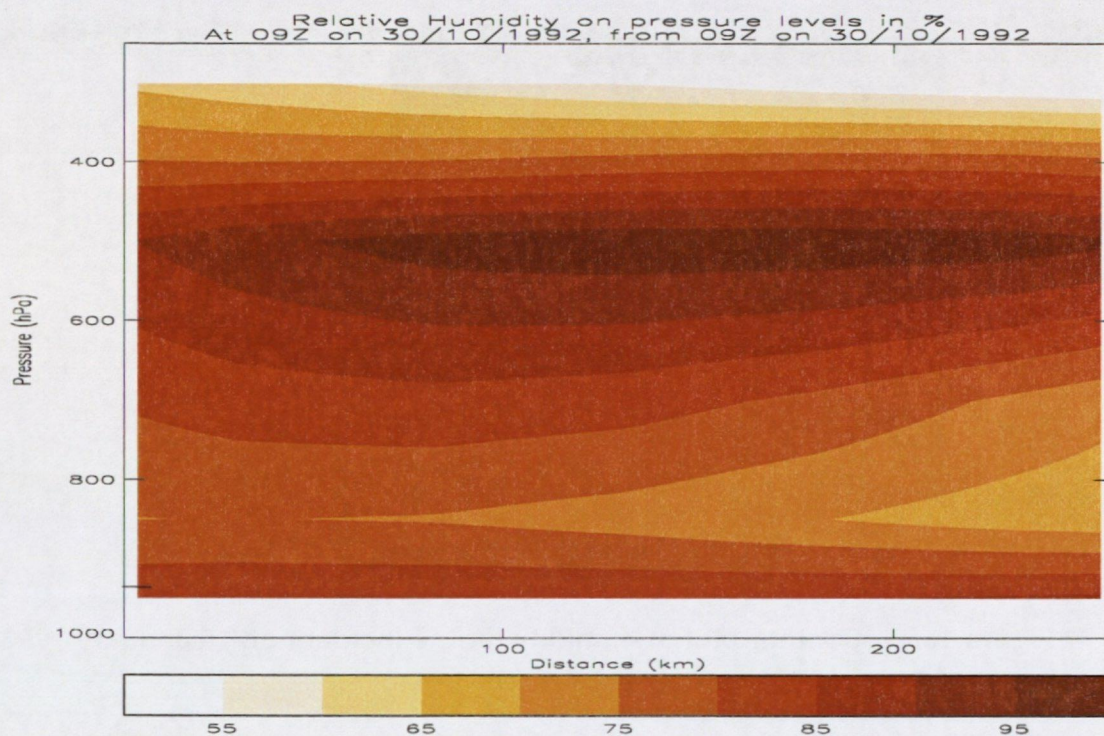


Figure 13: Contour plot of convective cloud depth for the incident on 30 October 1992



**Figure 14: Vertical cross-section of humidity for the incident on 30 October 1992**

3.2.2 *15 January 1993 at 16.00: 57.08°N 00.60°W: 2000 ft*

The NWP temperature data show this incident to be the warmest of the 11, with the air surrounding the helicopter at 278 K. The air was cooler to the west over the land and warmer to the east towards the coast of Norway. The winds were very strong at 28–30 m s<sup>-1</sup> and were in a west-south-westerly direction. The helicopter incident occurred where humidity was in the range 60–65%. The air was drier to the south but moister to the north where a region of air in the 85–90% humidity range stretched down in a north-east to south-west direction across Lerwick to central and western Scotland, see Figure 15. Ascending air was present to the east of the incident and the presence of convective cloud roughly coincided with the region of moist air just described above. The deepest cloud was between 500–600 hPa deep. The helicopter itself was clear of convective cloud.

The humidity profile shows a layer of moist air (70–80%) between 900 and 800 hPa to the north-north-west of the incident location. Above that, the humidity dropped again to 50–60%. The vertical velocity profile is shown in Figure 16. Descending air was present above and to the south-south-east of the incident. Ascent can be seen above the incident at about 600 hPa and at lower altitudes to the north-north-west.

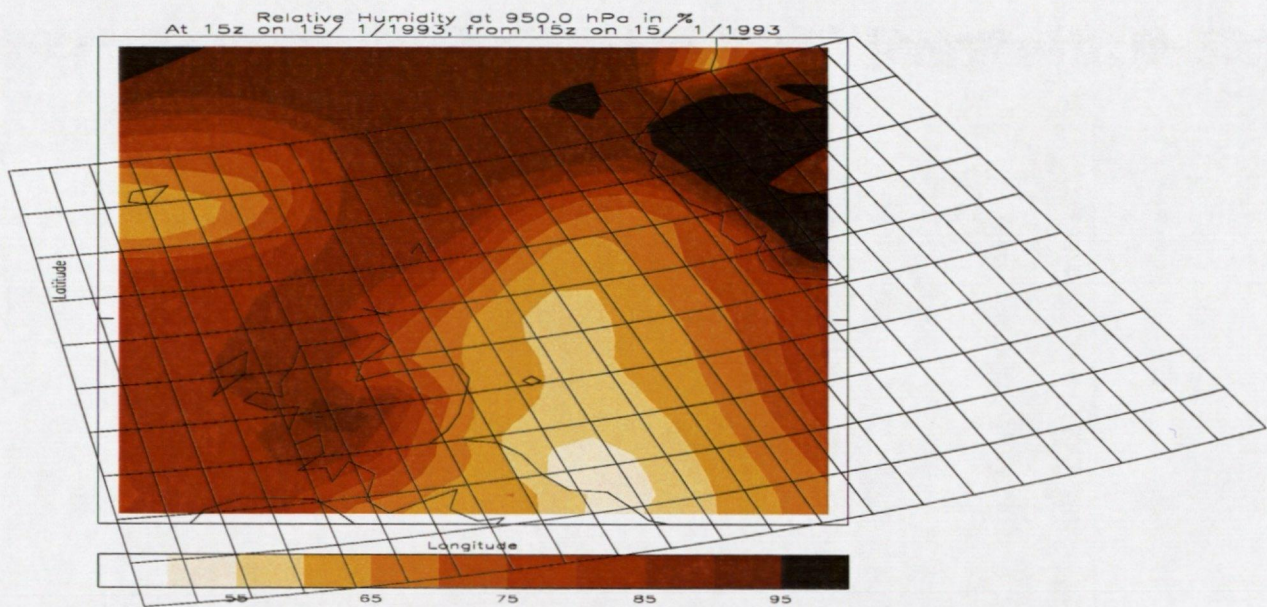


**Figure 15: Contour plot of humidity for the incident on 15 January 1993**

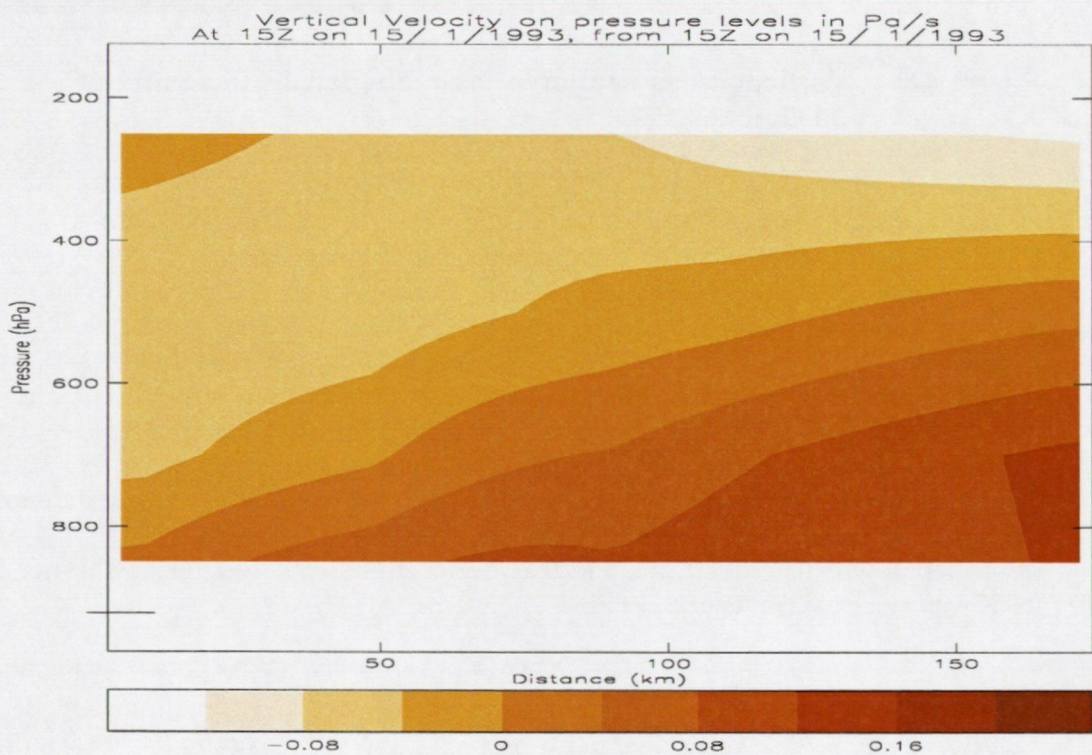


**Figure 16: Vertical cross-section of vertical velocity for the incident on 15 January 1993**

3.2.3 18 February 1993 at 17.06: 60.17°N 1.2°E: 2000 ft

The helicopter altitude coincided with the 275 K contour. A large area of air with uniform temperature in the range 274–275 K lay to the north and west. The air was warmer to the south and east. Wind speeds were in the range 18–20 m s<sup>-1</sup>, and the wind direction was north-westerly. Winds were stronger to the west and weaker to

the east. The humidity of the air surrounding the helicopter was in the range 75–80%, but increased to 95% over Norway. Drier air existed to the south-west. The helicopter lay on the edge of the  $0 \text{ Pa s}^{-1}$  contour and so was at the point where ascending and descending air met, as can be seen from Figure 17. There was ascending air to the north and west, and descending air to the south and east. Convective cloud was between 300 and 400 hPa deep, with the deepest area being to the north-west and having a depth of between 600 and 700 hPa.

The humidity vertical profile, Figure 18, shows 70–80% humidity at the incident altitude. There was a layer of dry air (50–60%) at 850 hPa, with moister air above. At higher levels (500 hPa) there was moister air to the north end of the profile and dryer air to the south. The vertical velocity profile shows that ascent was widespread to the north and above 825 hPa. There was descent at lower altitudes to the south of the incident.

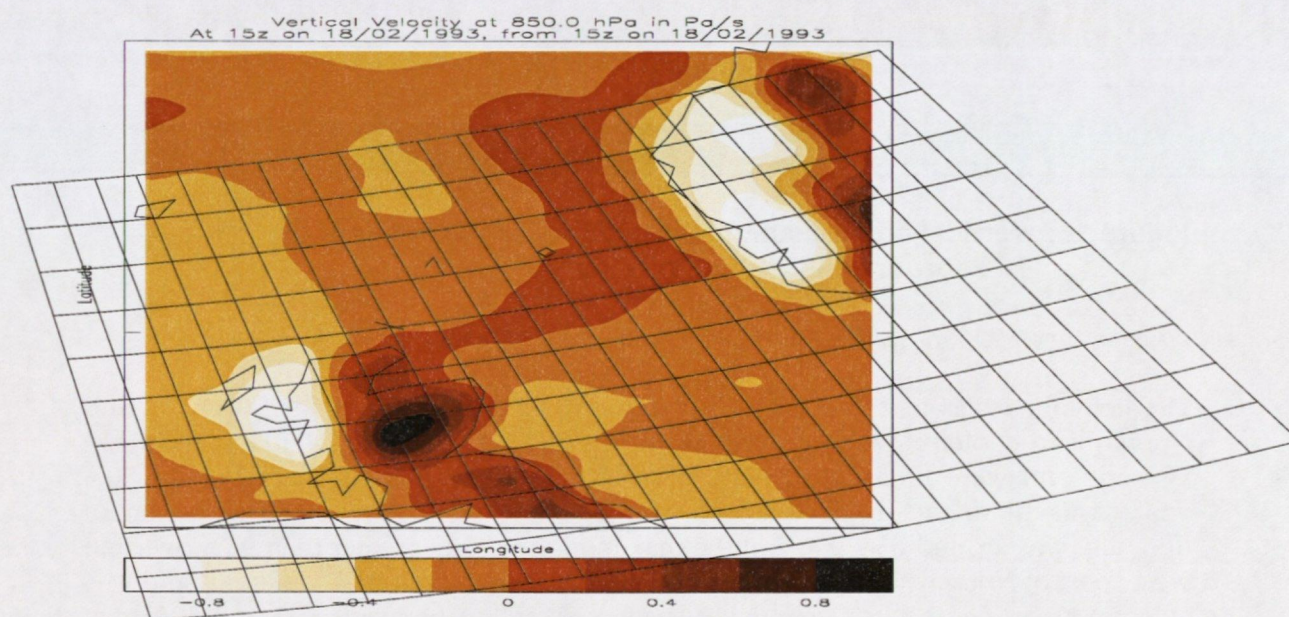


**Figure 17: Contour plot of vertical velocity for the incident on 18 February 1993**

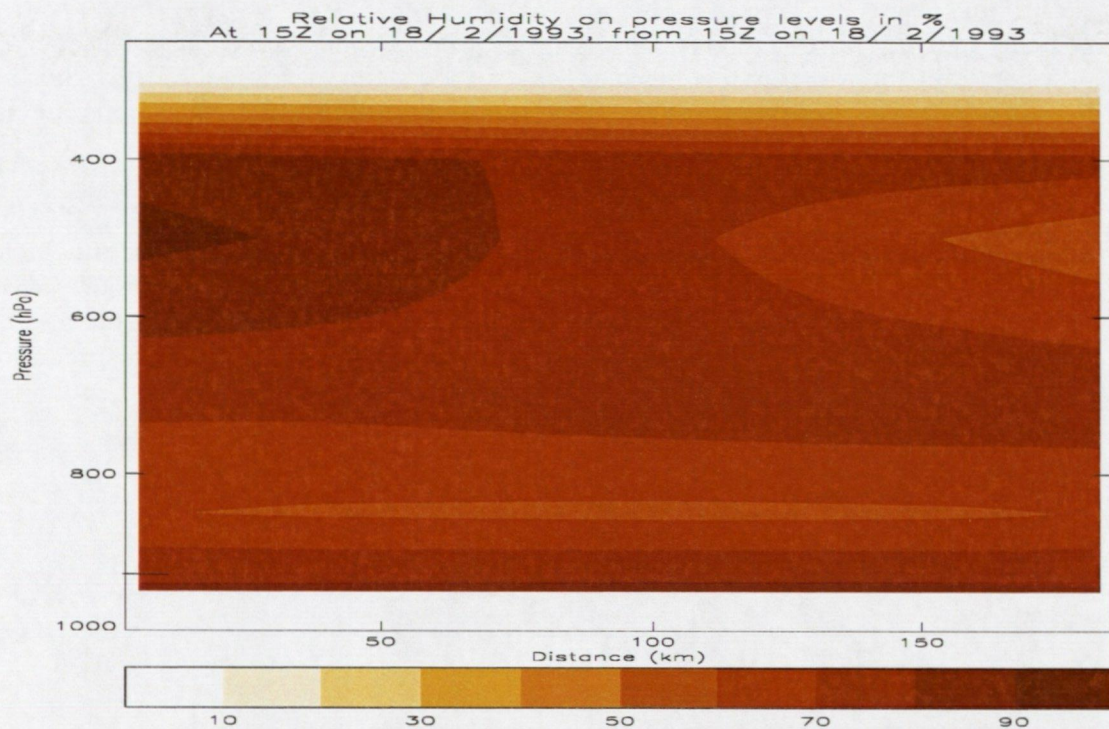


**Figure 18: Vertical cross-section of humidity for the incident on 18 February 1993.**

3.2.4 *20 February 1993 at 11.25: 60.08°N 1.05°W: 3000 ft*

The helicopter was in 275 K air with warmer air to the south between Scotland and Norway and cooler air to the north, as shown in Figure 19. The winds were north-westerly and were uniformly 24–28 m s<sup>-1</sup>. The humidity was in the range 75–80% with dryer air to the north-west and moister air to the south-east. The minimum humidity was around 65–70%, and the maximum humidity greater than 95% over the west coast of Norway. The helicopter was again close to the 0 Pa s<sup>-1</sup> contour, and was in convective cloud with a relatively shallow depth of between 200 and 300 hPa. There was deeper cloud to the north-east.

The vertical cross-section of humidity shows a dry layer (40–50%) at 300 hPa and moist air (80–90%) from 700 hPa down to the surface. There was widespread ascent, see Figure 20, with the only descent occurring in the highest model level (at around 250 hPa).

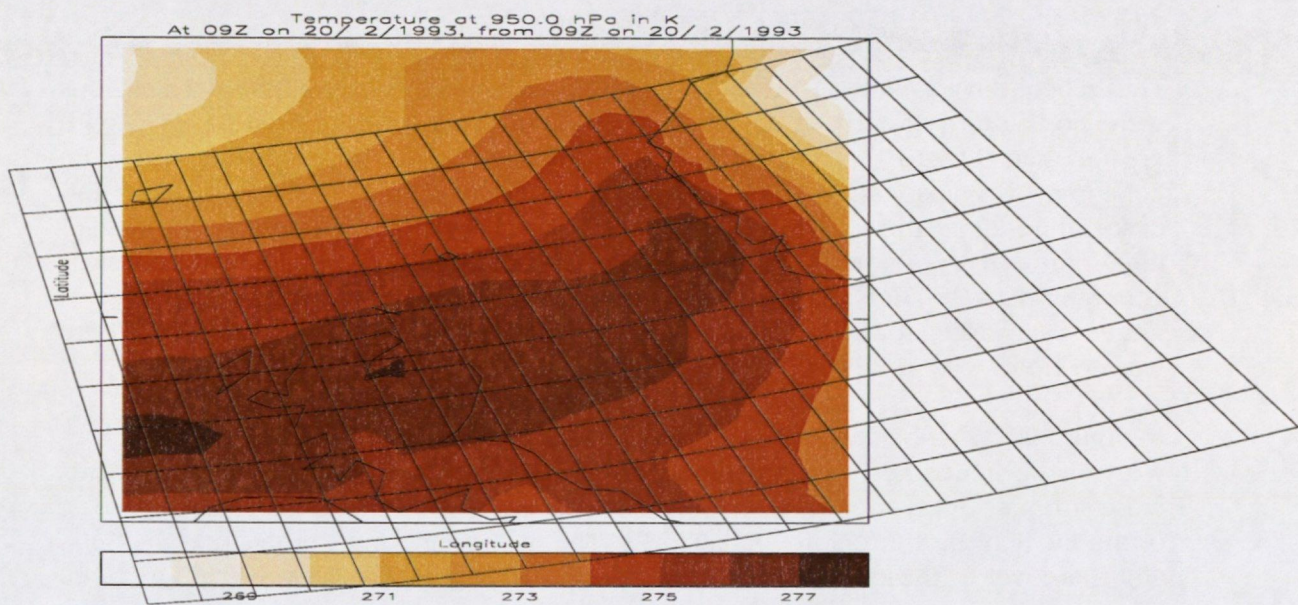


Figure 19: Contour plot of temperature for the incident on 20 February 1993

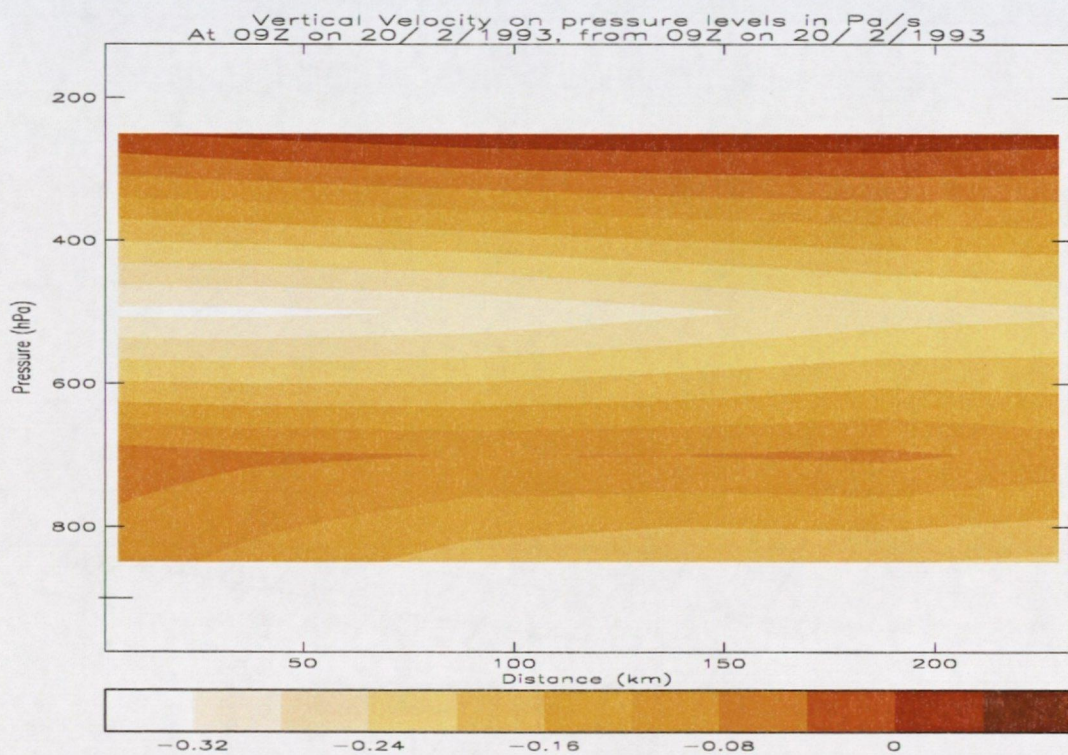


Figure 20: Vertical cross-section of vertical velocity for the incident on 20 February 1993

3.2.5 3 October 1994 at 13.50: 60.30°N 00.32°E: 1500 ft

The helicopter was very close to the 273 K contour (the freezing level). The winds were north-north-easterly at 16–18 m s<sup>-1</sup>. Humidity was in the range 80–85%, with greater than 90% to the north, 85–90% to the west, and 70–75% to the east. The helicopter was close to the 0 Pa s<sup>-1</sup> contour, with ascending air to the north-west and descending air to the south-east. The incident occurred to the south of an area of high convective rain rate with a cell-like structure. The convective cloud was generally between 300 and 400 hPa deep but was deeper than this to the north-east. There was a large area of cloud ice to the north, as can be seen from Figure 21. There was no cloud water in the vicinity.

In Figure 22 it can be seen that the winds were weaker above and to the west-south-west of the helicopter, but at higher altitudes and to the east-north-east the winds were stronger. A layer of dryer air (50–60%) existed above and to the east-north-east of the incident in the region 700–600 hPa. The air became moister again at the 500–400 hPa level to the east-north-east. There was strong ascent between 950 and 700 hPa to the east-north-east. Again, the incident was close to the point where ascending and descending air met.

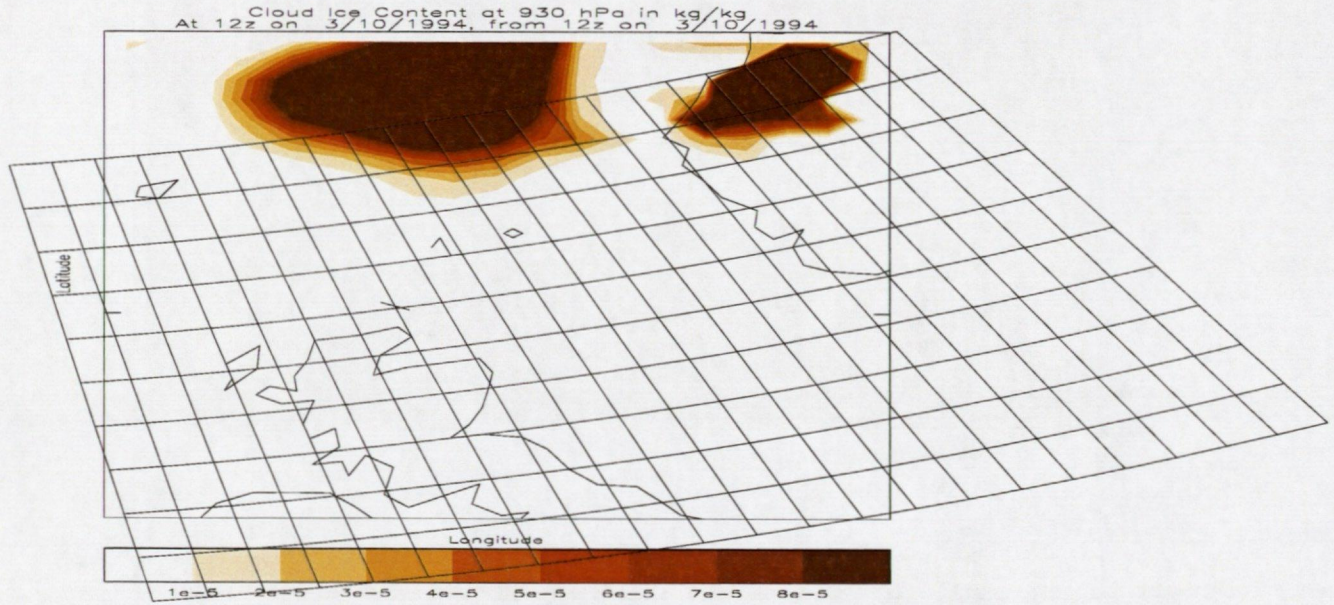
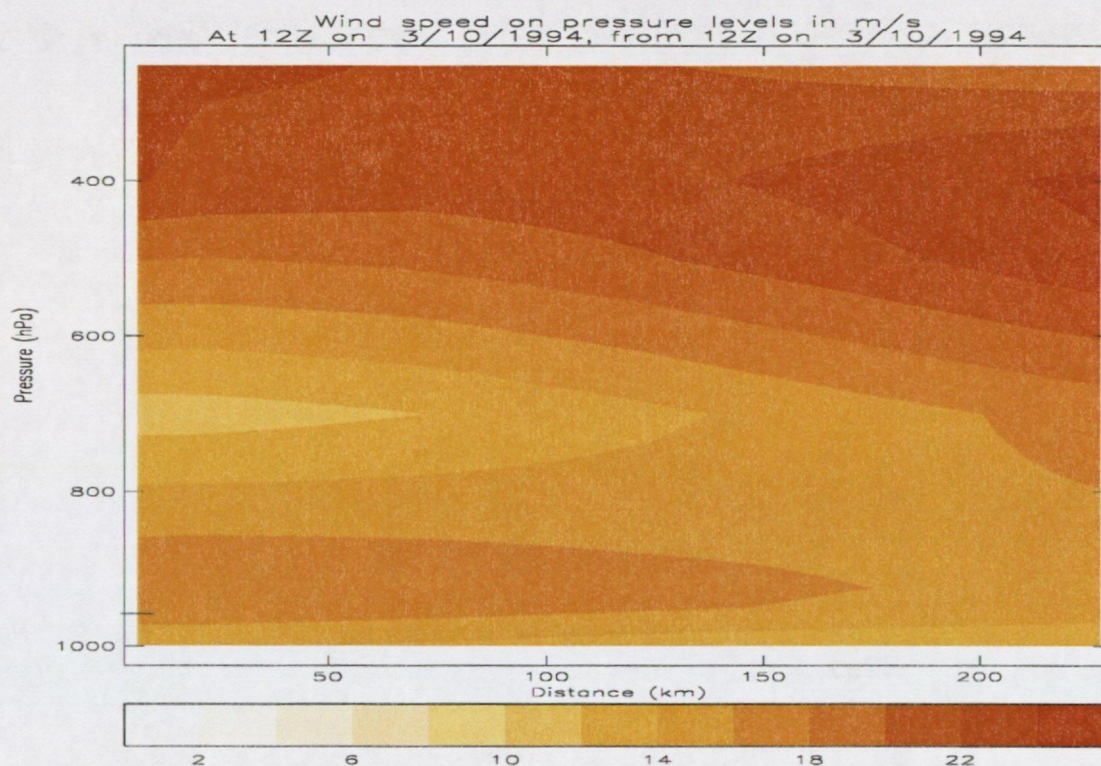


Figure 21: Contour plot of cloud ice content for the incident on 3 October 1994



**Figure 22: Vertical cross-section of wind speed for the incident on 3rd October 1994**

3.2.6 19 January 1995 at 12.34: 58.47°N 00.85°E: 3000 ft

The air was warmer to the east and cooler to the west of the incident, with south-westerly winds at 16–18 m s<sup>-1</sup>. Humidity was greater than 90% with dryer air to the south and west. The helicopter was in an area of ascending air but was very close to the 0 Pa s<sup>-1</sup> contour. The incident was on the edge of an area of high convective rain rate, which took the form of 3 cells, as shown in Figure 23. Convective cloud was coincident with the high convective rain rate, with the deepest cloud between 400 and 500 hPa deep. The incident was just to the north-east of a small area of cloud ice. No cloud water was present.

In the vertical the winds increased with altitude and to the east. A moister layer of air existed below the incident with much dryer air above the incident and to the west. The vertical velocity profile in Figure 24 clearly shows ascending air to the east and descending air to the west, with the helicopter being positioned between them. Cloud ice existed only at the same level as the helicopter and to the west. There was no cloud water.

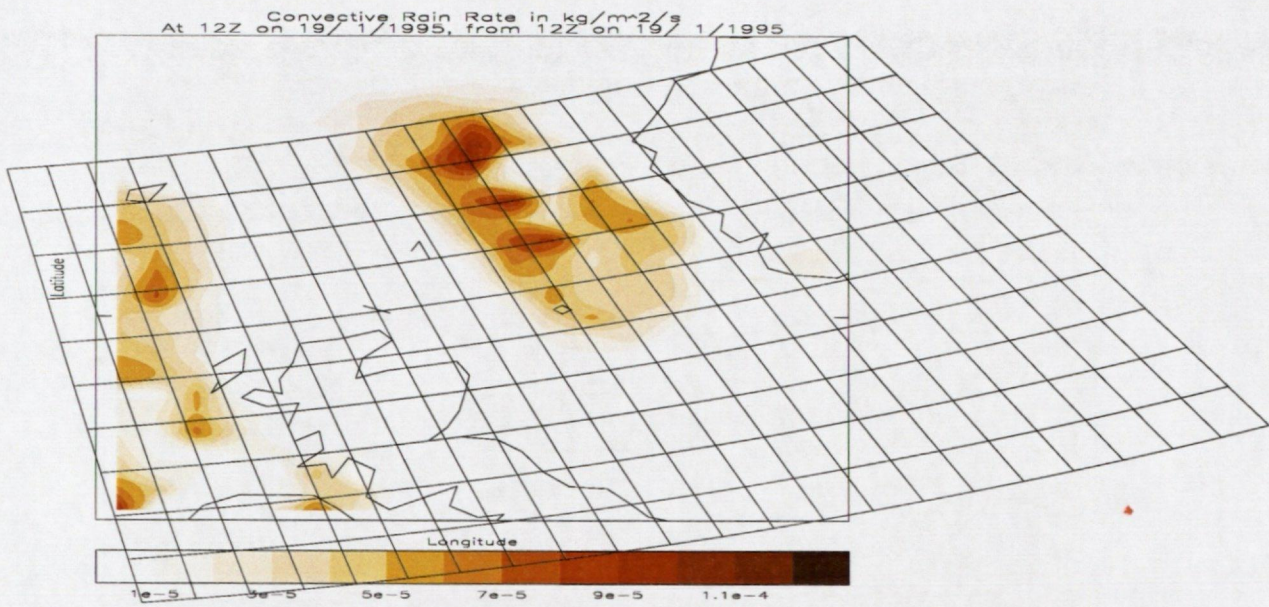


**Figure 23: Contour plot of convective rain rate for the incident on 19 January 1995**

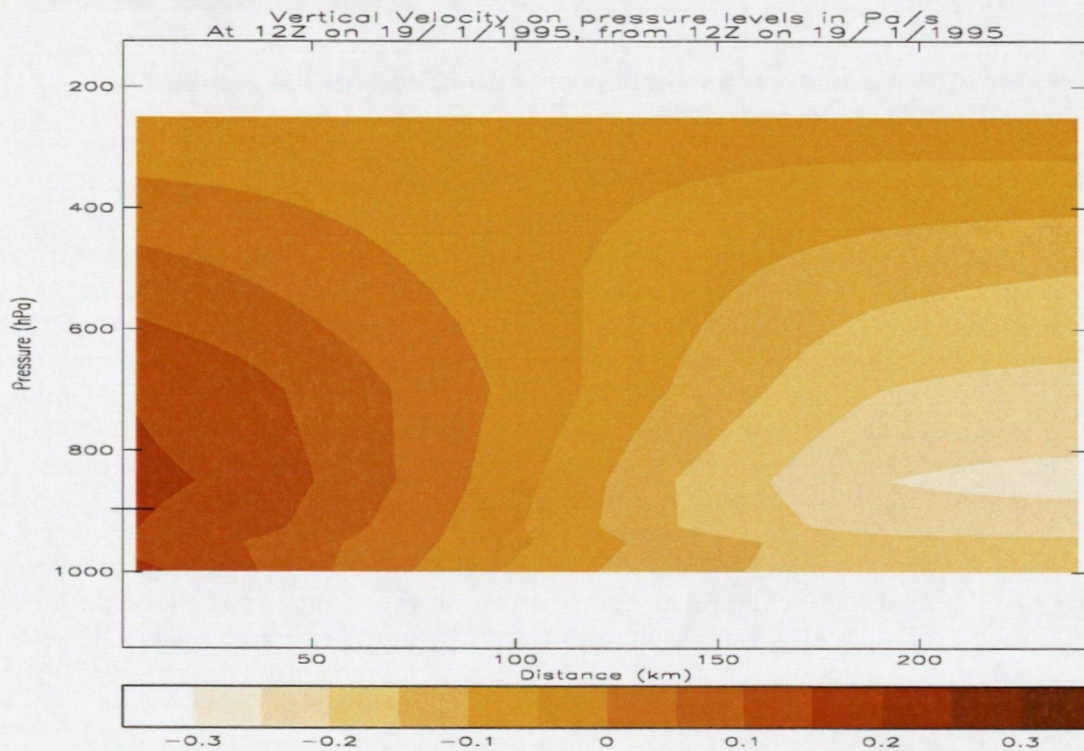


**Figure 24: Vertical cross-section of vertical velocity for the incident on 19 January 1995.**

3.2.7 21 February 1995 at 09.18: 59.33°N 1.00°E: 2000 ft

The helicopter was in air with temperature in the range 273–274 K. The wind was light and from the south-west. The incident occurred just to the north-east of a dryer region of air where the humidity was less than 60%, as shown in Figure 25. Moister air existed to the north-west, north-east and south-east. The helicopter was clear of both convective cloud and convective rain, with the positions of the convective cloud and rain being coincident. The deepest clouds were to the north-west and were between 600 and 700 hPa deep. The helicopter was clear of cloud ice and water.

The air surrounding the helicopter had humidity in the range 70–80%. This humidity increased with altitude and to the south-east. The helicopter was in ascending air, with descending air at 1000–950 hPa to the south-east. The magnitude of the ascent increased with altitude and to the south-east. There was no cloud ice or cloud water. Wind speed increased with altitude as was typical. This is shown in Figure 26.

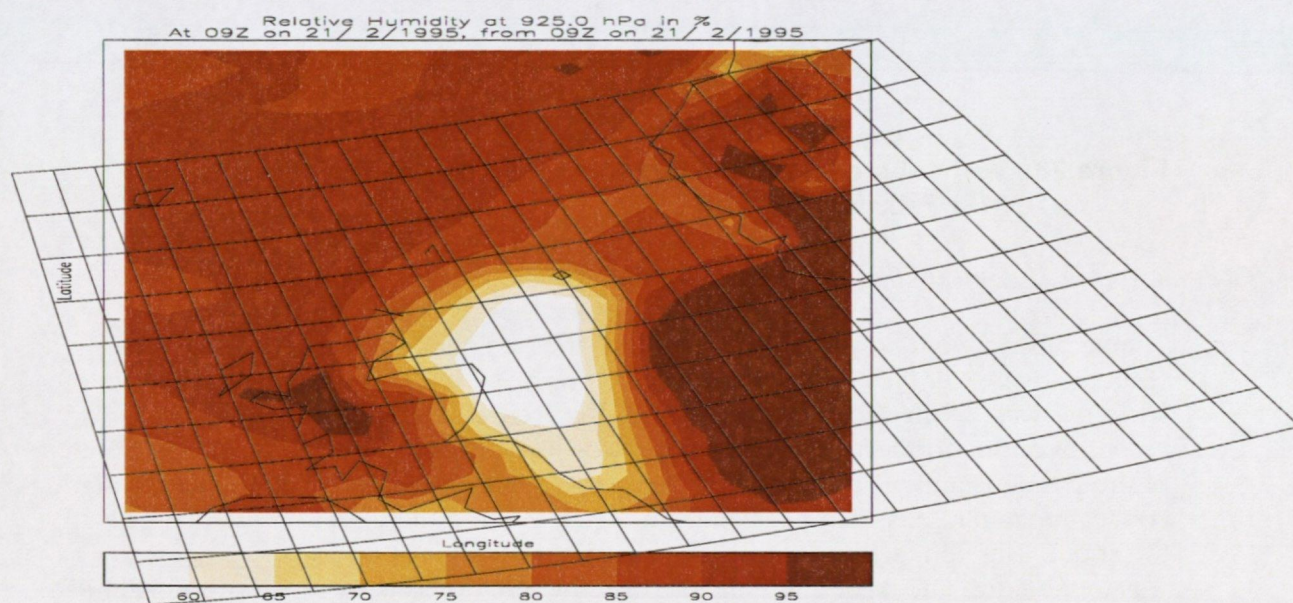
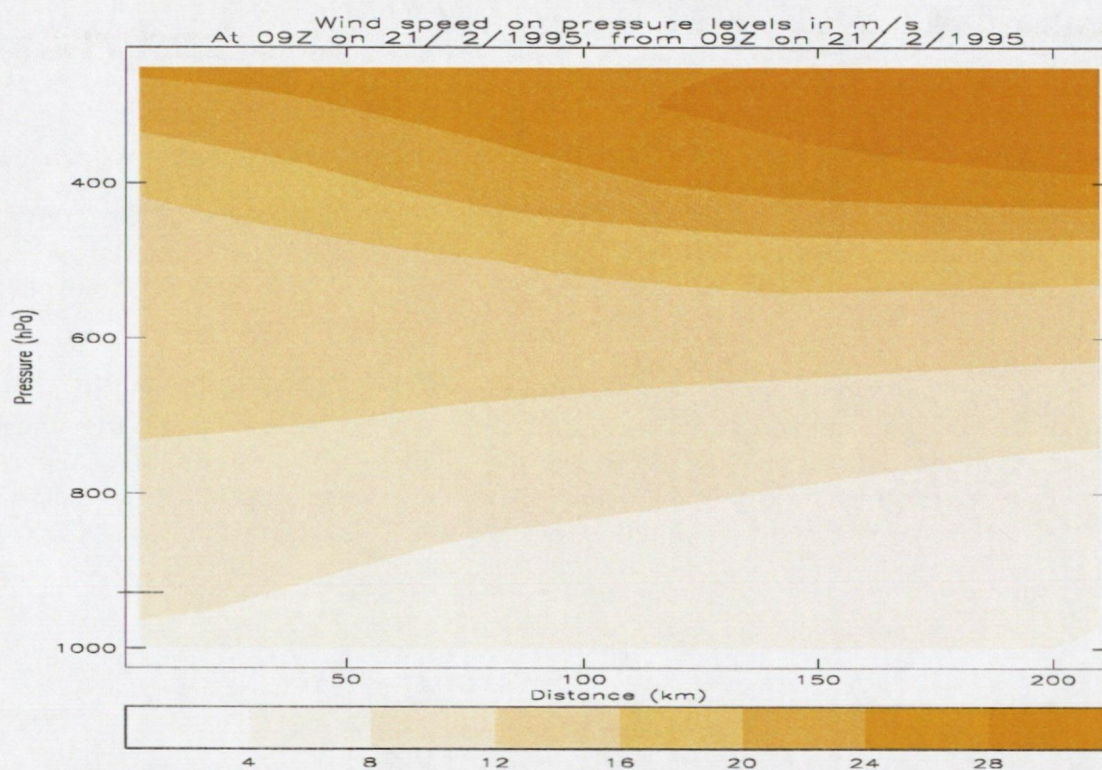


Figure 25: Contour plot of humidity for the incident on 21 February 1995.



**Figure 26: Vertical cross-section of wind speed for the incident on 21st February 1995**

3.2.8 1 March 1995 at 09.07: 60°N 1.00°W: 2000 ft

Temperatures were lower to the west of the incident. The wind was westerly. Humidity was over 90% across the northern North Sea but there was a drier pocket of air to the west of the incident just south of the Færoe Islands. There was widespread ascent over the northern North Sea but descent coincident with the drier area south of the Færoe Islands. The incident occurred on the southern edge of an area of high convective rain rate, as can be seen from Figure 27, and there were more rain cells to the south. The convective cloud base was at about 800–900 hPa. The deepest cloud was to the north and west of the incident site, where it was between 400 and 500 hPa deep. The incident was on the edge of an area of cloud ice, which was located to the south and west.

In the vertical the wind was uniformly 12–16 m s<sup>-1</sup>. The humidity at the height of the helicopter was in excess of 80% but above that there existed a layer of dryer air and higher yet another layer of moister air with a humidity of greater than 90%. Ascent was occurring over the incident site with descent occurring to the north and south. There was a small amount of cloud ice at 500 hPa and to the south of the incident around 950–900 hPa, as shown in Figure 28. No cloud water was present.

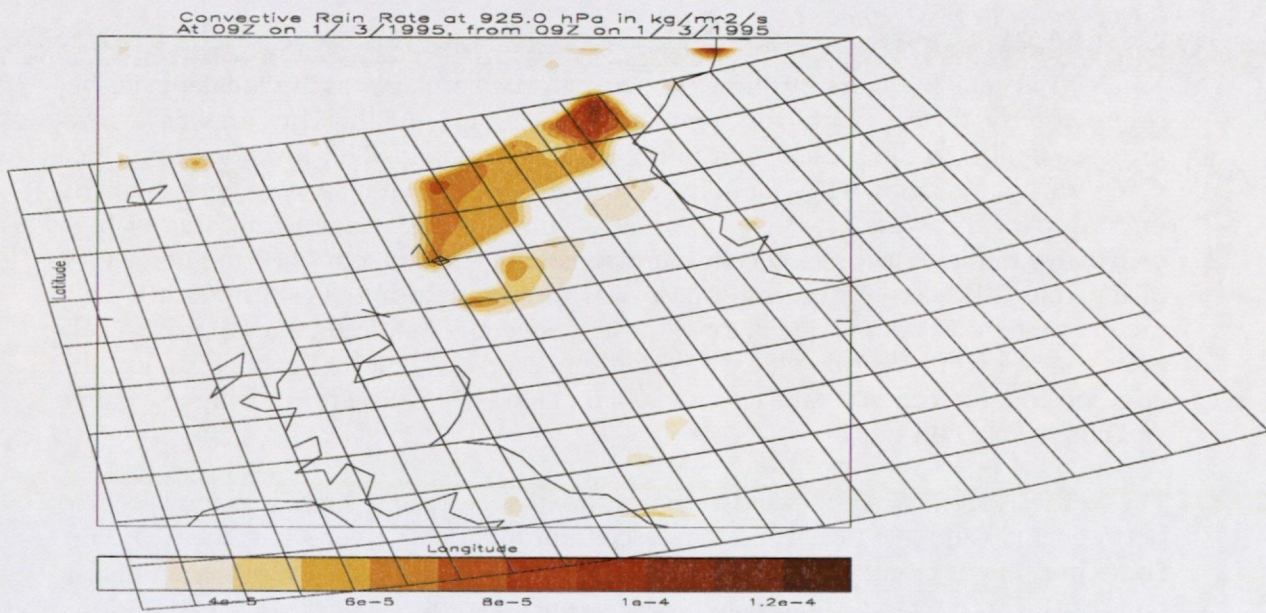


**Figure 27: Contour plot of convective rain rate for the incident on 1 March 1995**

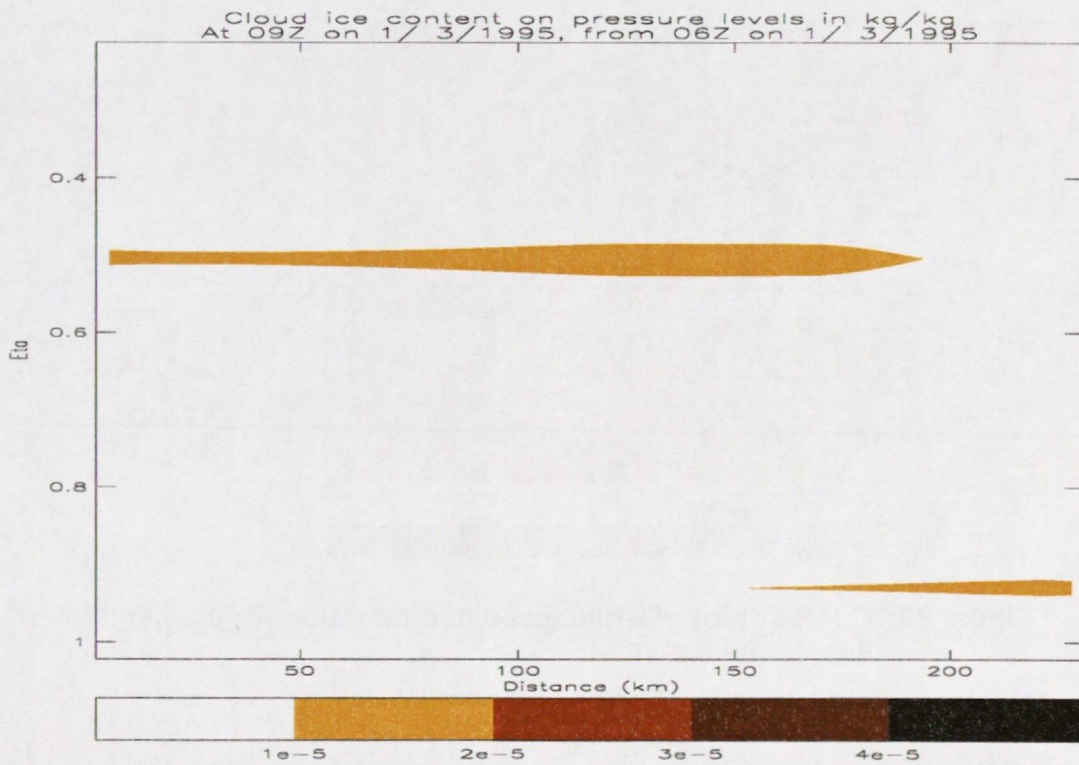


**Figure 28: Vertical cross-section of cloud ice for the incident on 1 March 1995**

3.2.9 8 December 1995 at 10.48: 60.33°N 00.33°E: 2000 ft

The NWP results in Figure 29 show the winds to be southerly at the incident site but south-easterly to the north and south-westerly to the south. This implies a low-pressure centre to the west of the north coast of Scotland. The northern North Sea was very humid with 95% humidity across the whole area. Ascent was similarly uniform over the same area. The incident occurred on the edge of an area of high convective rain rate in which 9 cells were apparent. The incident occurred between 2 of the cells. The convective cloud base was uniformly at about 900–1000 hPa with the deepest cloud being coincident with the convective rain rate, and approximately bisecting the North Sea between Scotland and Norway. The helicopter was on the edge of a large area of cloud ice, which coincided with the areas of high dynamic and convective rain rate.

The vertical profiles show winds stronger to the east, and high humidity (>95%) between 1000 and 350 hPa. There was ascent throughout the vertical velocity profile. Some pockets of cloud ice were present above the helicopter location, as shown in Figure 30. There was no cloud water close to the incident.

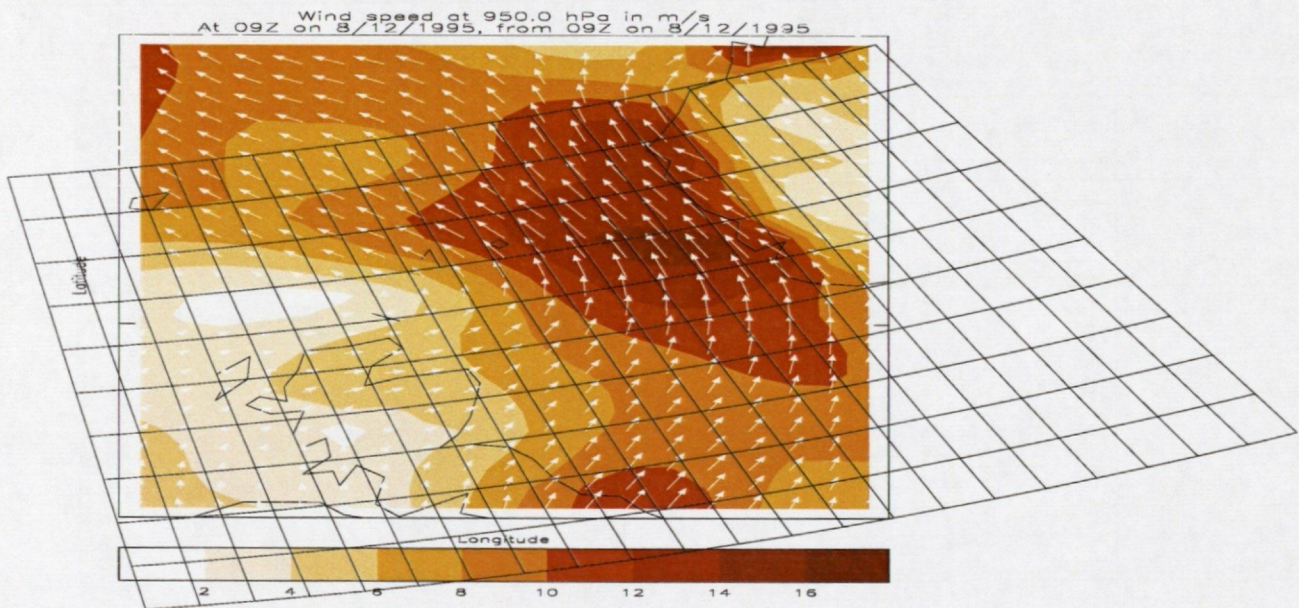
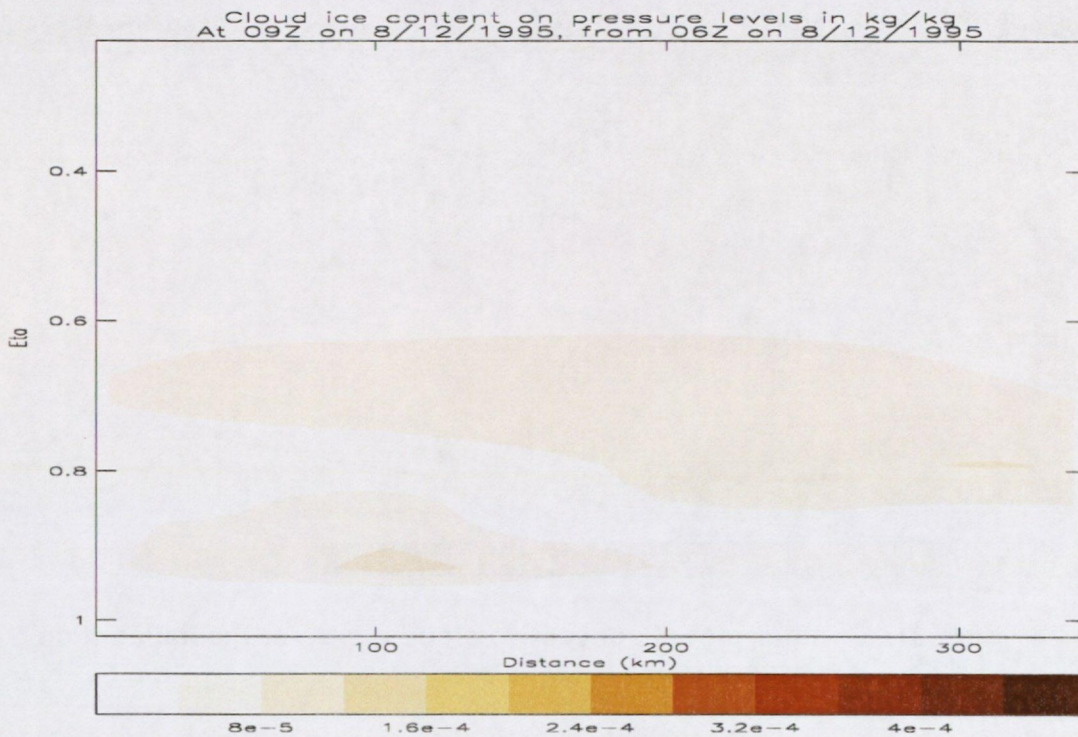


Figure 29: Contour plot of wind speed and direction for the incident on 8 December 1995



**Figure 30: Vertical cross-section of cloud ice for the incident on 8 December 1995**

3.2.10 8 February 1996 at 10.30: 60.68°N 1.25°E: 1500 ft

A contour plot of temperature shows that it was colder to the east and warmer to the west of the incident. The winds were southerly at  $12 \text{ m s}^{-1}$ . An area of moist air ( $>94\%$ ) surrounded the incident, with much drier areas ( $<72\%$ ) over the west coast of Norway and to the north of Scotland. Air was ascending over the incident site but to the north-east and south-west the air was descending. The incident occurred between 2 areas of convective rain. The cloud base was uniformly at 900–1000 hPa, with cloud depth of about 300 to 400 hPa, as can be seen from Figure 31. This cloud was coincided with the convective rain. Cloud ice was present to the south of the incident at 06 UTC but none was present at 09 UTC.

The wind profile shows a core of high winds ( $20 \text{ m s}^{-1}$ ) at approximately 350 hPa. A region of high humidity ( $>95\%$ ) existed to the west of the incident between 800–300 hPa and another smaller region existed between 950–900 hPa. At higher levels this stretched eastwards up to 700 hPa over the incident site. The vertical velocity profile shows that the incident occurred very close to  $0 \text{ Pa s}^{-1}$ , and was therefore at a point where ascending and descending air met. Figure 32 shows that cloud ice existed to the west of the incident at 950 hPa, with lower concentrations higher in the atmosphere.

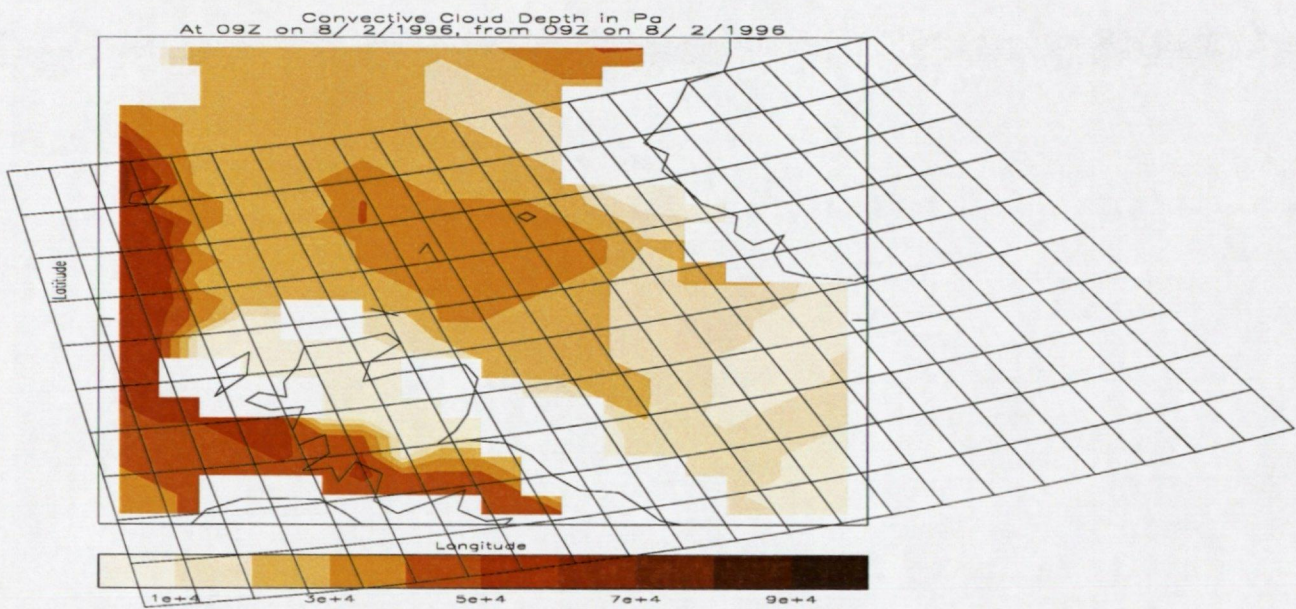


**Figure 31: Contour plot of convective cloud depth for the incident on 8 February 1996**

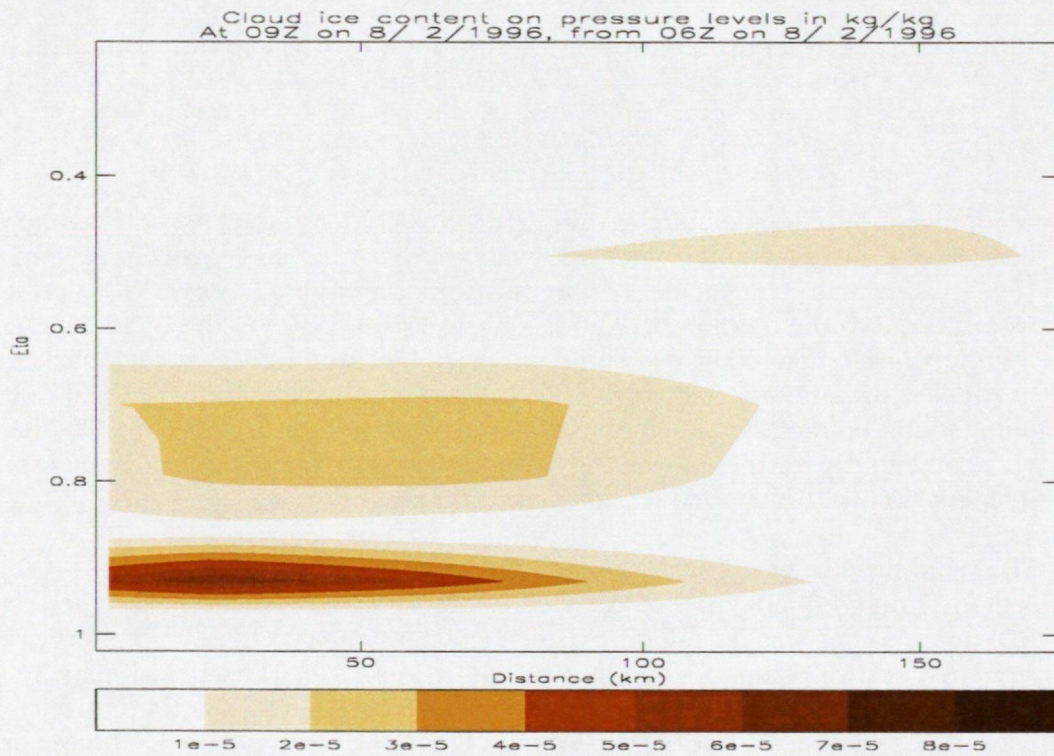


**Figure 32: Vertical cross-section of cloud ice for the incident on 8 February 1996**

3.2.11 26 November 1996 at 14.56: 53.85°N 1.42°E: 2000 ft

The temperature at the incident site was approximately 275 K. The wind was in an east-north-easterly direction. There was a moist (>90%) area to the west of the incident which could actually have been overhead at the time of the incident. The contour in Figure 33 dividing the ascending and descending air runs north to south through the incident site, with the descending air being moister than the ascending. A small area of convective rain was present to the north-east of the incident site. The convective cloud base over the North Sea was uniformly at 900 hPa but there was no convective cloud over the incident site. The deepest convective cloud was coincident with the highest convective rain rates. No cloud water or cloud ice was present.

The humidity was greater than 90% at the incident location but reduced to less than 10% between 500 and 400 hPa, as shown in Figure 34. The atmosphere was moister again above 400 hPa. The vertical velocity profile showed descent throughout the atmosphere. No cloud water or cloud ice was present.

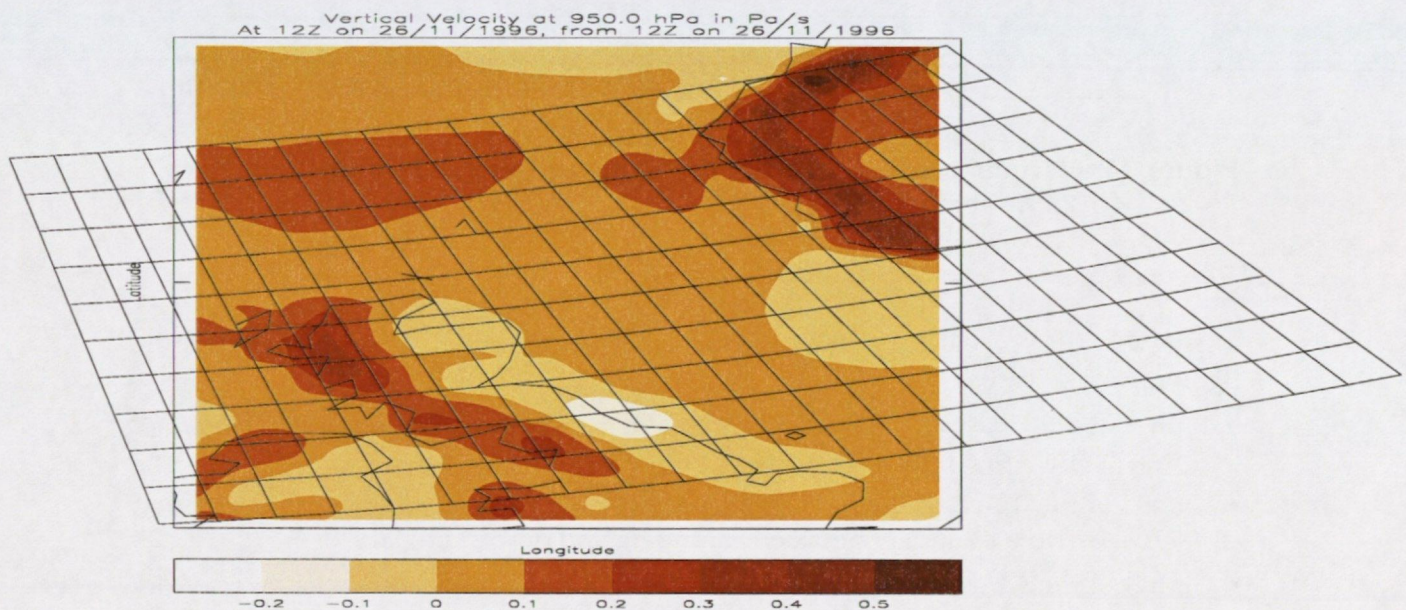
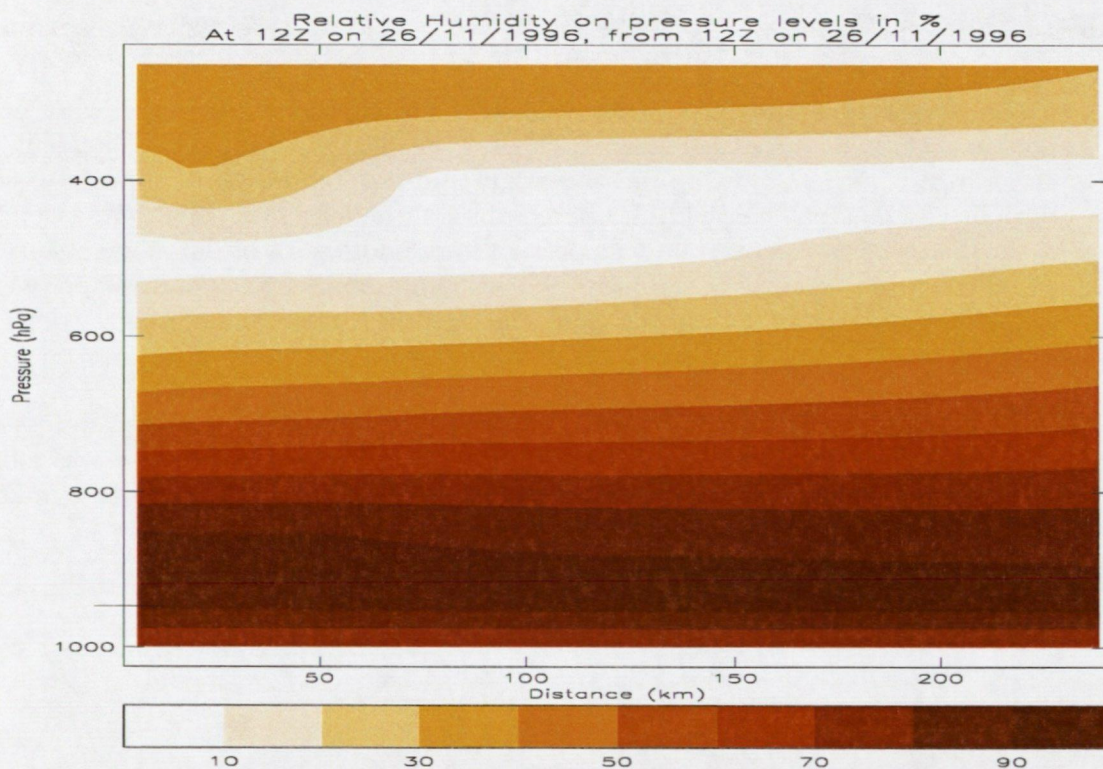


Figure 33: Contour plot of vertical velocity for the incident on 26 November 1996



**Figure 34: Vertical cross-section of humidity for the incident on 26 November 1996**

### 3.2.12 Summary

The NWP data revealed 3 characteristics that are common among some of the lightning strike cases.

- In 5 of the 7 cases for which convective rain rates were available, the helicopter was on the edge of high convective rain rate cells.
- In 6 of the 11 cases the helicopter was near a  $0 \text{ Pa s}^{-1}$  vertical velocity contour, i.e. close to a boundary between ascending and descending air.
- In 3 of the 11 cases the vertical structure of the humidity showed a layer of dry air between two layers of moist air. There were no obvious patterns in the humidity profiles for the other 8 cases.

## 4 QUANTITATIVE RESULTS

### 4.1 Sferics

Sferic data for the 11 incidents are summarised in Table 2, which contains the location and time of each incident, the location and time of the sferic nearest to the incident locality, and the total number of sferics within 400 km of the incident on the day in question. For 7 of the incidents, marked in the table with an asterisk, there was a good spatial and temporal match between the incident and the nearest sferic, with the incident occurring within 10 nautical miles and 8 minutes of the sferic. The locations and times of the incident reports were considered to be of this accuracy. For 3 of the other incidents no good match was found and for the 1992 incident sferic data were unavailable.

Date	Incident			Nearest sferic			Sferics	
	Latitude	Longitude	Time	Latitude	Longitude	Time		
26/11/96	53.85	1.42 E	14.56	53.90	1.50 E	14.53	1	*
08/02/96	60.68	1.25 E	10.30	60.75	1.45 E	10.22	1	*
08/12/95	60.33	0.33 E	10.48	60.62	0.20 W	10.44	34	
01/03/95	60.00	1.00 W	09.07	60.02	0.85 W	09.05	49	*
21/02/95	59.33	1.00 E	09.18	59.47	1.20 E	09.13	15	*
19/01/95	58.47	0.85 E	12.34	58.47	0.95 E	12.29	307	*
03/10/94	60.30	0.32 E	13.50	59.35	2.15 E	14.03	3	
20/02/93	60.08	1.05 W	11.25	60.00	1.05 W	11.19	42	*
18/02/93	60.17	1.20 E	17.06	60.67	1.10 E	17.03	11	
15/01/93	57.08	0.60 W	16.00	56.97	0.55 W	15.55	167	*
30/10/92	60.97	1.42 E	10.04				27	

**Table 2: Temporal and spatial match between helicopter lightning strikes and observed sferics. Sferics marked with an asterisk are a good match with the strike. Sferic data were unavailable for the 1992 incident**

It can be seen from Table 2 that there was a great deal of variability in the total number of sferics, with a minimum of 1 and a maximum of 307. In the latter case the location and time of the incident could have been predicted as being of high risk because of the large number of sferics that were observed in the vicinity just prior to the incident. Similar predictions could not have been made for the other incidents.

It is believed that the 2 cases in 1996 were triggered by the helicopter. Only 1 sferic was recorded on each of these days and it was a good spatial and temporal match with the incident.

Sferic data were also retrieved for an incident on 26 February 1996 for which the only location given on the pilot report was '35 n mile east of?'. Just 1 sferic was detected on this day and it was at the exact time of the incident 35 n mile east of Sumburgh. Despite this finding the incident was not studied further.

#### 4.2 Convective cloud (from synoptic charts)

All of the lightning strike incidents occurred between October and March and so it was thought that there might be a relationship between the convective cloud base and the month of the year, with the cloud base being lower during the winter.

Observations of cloud base made hourly at Lerwick and Hemsby during 1997 were examined. The monthly mean cloud base and the total number of cloud base observations contributing to that mean are plotted in Figures 35 and 36 as a function of the month, for Lerwick and Hemsby respectively. The total number of cloud base observations depends on the amount of convective cloud present during each month. It can be seen that there was no monthly variability in the cloud base at Lerwick. However at Hemsby there was slight variability, with the cloud base being marginally higher during the summer months.

The lack of variability in the cloud base on a month to month basis was unexpected. Since the cloud base measured by a human observer could be subjective, the cloud base was re-examined using a more objective approach that involved the dew-point depression.

Dew-point depression is a useful indicator of the moistness of the atmosphere. It is the difference at the surface between the temperature and the dew-point temperature, where dew-point temperature is the temperature to which air has to be cooled for it to become saturated. When the dew-point depression is zero the air is saturated and water vapour condenses to form cloud. Since air cools with increasing altitude, the smaller the dew-point depression the lower the cloud base is likely to be.

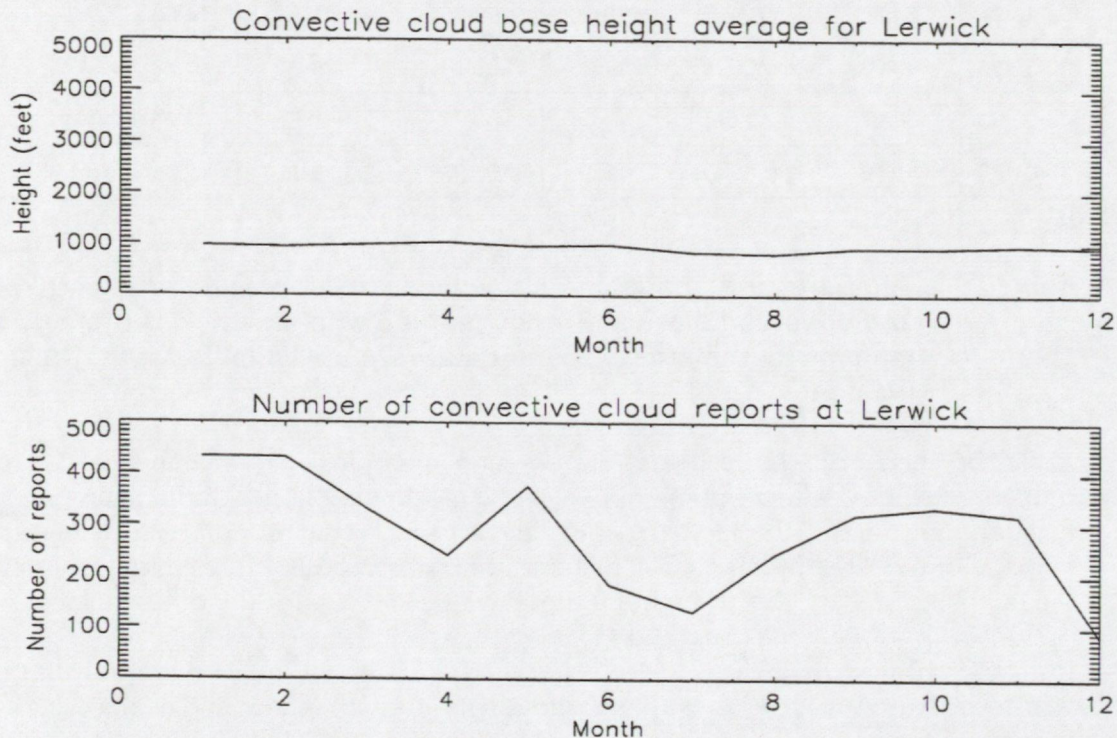


**Figure 35: Monthly mean of the convective cloud base (top graph) and the number of observations contributing to that mean (bottom graph) for Lerwick in 1997**

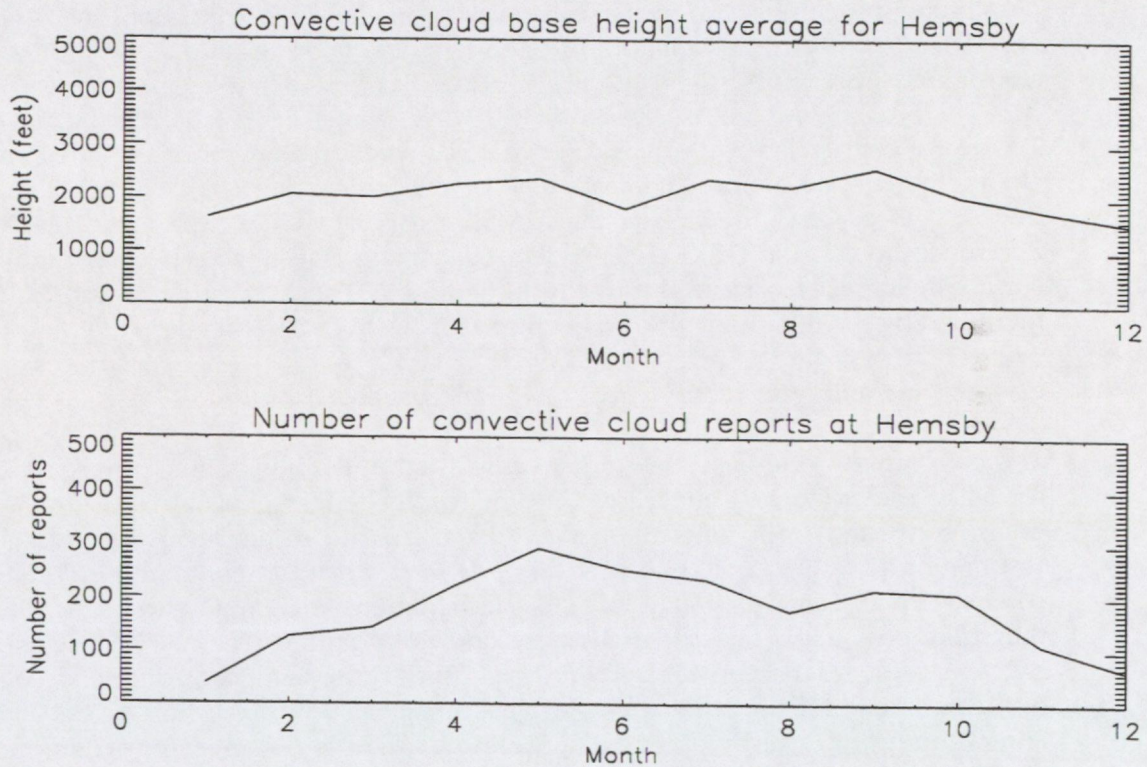


**Figure 36: Monthly mean of the convective cloud base (top graph) and number of observations contributing to that mean (bottom graph) for Hemsby in 1997**

The monthly mean and monthly standard deviation of the dew-point depression are plotted in Figures 37 and 38 as a function of the month, for Lerwick and Hemsby respectively, for 1997. The figures show that the monthly mean dew-point depression did change from month to month for both Lerwick and Hemsby. However the changes in the monthly means were mirrored by changes in the monthly standard deviations, suggesting that the changes in the monthly means were due to a few large values of dew-point depression, rather than a more general trend.

There is thus no evidence to suggest that the convective cloud base in the North Sea is lower in the winter than in the summer.

#### 4.3 Convective cloud (from radiosonde ascents)

Temperatures and dew-point temperatures obtained during a radiosonde ascent can be displayed and interpreted on a thermodynamic diagram known as a tephigram. Details of tephigram use will not be given here, but interested readers are referred to the Handbook of Aviation Meteorology (Met. Office 1994).

Tephigrams are invaluable for understanding convective cloud. Useful quantities that can be calculated from a tephigram include the freezing level, the convective cloud base, the cloud depth, and the Convective Available Potential Energy (CAPE).

CAPE is the amount of energy available in the atmosphere for powering convection, and it depends on the temperature lapse rate and the moisture content of the atmosphere. A high value of CAPE implies high updraft velocities within a cloud, since the maximum updraft velocity is proportional to the square root of CAPE, and high updraft velocities can lead to significant electric charge separation and the

possibility of lightning. For further information on cloud electrification, see Weber et al. (1993) for a brief explanation, or Saunders (1995) or Volland (1995) for a more complete overview.

To ensure consistency with the presence of convection as recorded on the synoptic charts, the surface temperatures of some of the radiosonde ascents were altered in line with forecasting practice so that CAPE was greater than zero (The Forecasters' Reference Book (Met. Office 1997)). This adjustment is justifiable because significant surface heating can occur during daylight hours. The surface temperatures were increased by the minimum amount required for CAPE to be non-zero.

#### 4.3.1 *Convective cloud base, cloud depth, CAPE and helicopter altitude*

The convective cloud base, freezing level, cloud depth and CAPE are given in Table 3 for all of the strike and null cases. The helicopter height is also given for the strike cases, converted from units of feet to hPa using the mean sea level pressure and assuming a pressure lapse rate of 1 hPa per 30 ft. The data contained in Table 3 are summarised in Table 4, which contains the minimum, maximum and mean values for the strike cases, the Lerwick null cases, and the combined Lerwick & Hemsby null cases. A t-test on the convective cloud base shows no significant difference between the mean value for the strike cases and the mean value for the null cases, both with and without the Hemsby null cases. The same result is obtained for t-tests involving the freezing level, the cloud depth and the CAPE.

The convective cloud base, freezing level and helicopter height for each strike case are plotted in Figure 39. For each case there are 6 possible orderings of these parameters in the vertical, but as can be seen from the figure that only 4 of the orderings actually occurred. A schematic picture of these 4 orderings is given in Figure 40, together with their corresponding CAPE values. For 8 of the incidents the helicopter was below the convective cloud base and for the remaining 3 incidents it was 20–40 hPa (600–1200 ft) above the convective cloud base. It is also worth noting that for 7 of the 11 incidents the entire cloud was below freezing. There is no apparent relationship between the CAPE values and the orderings of the convective cloud base, freezing level and helicopter height.

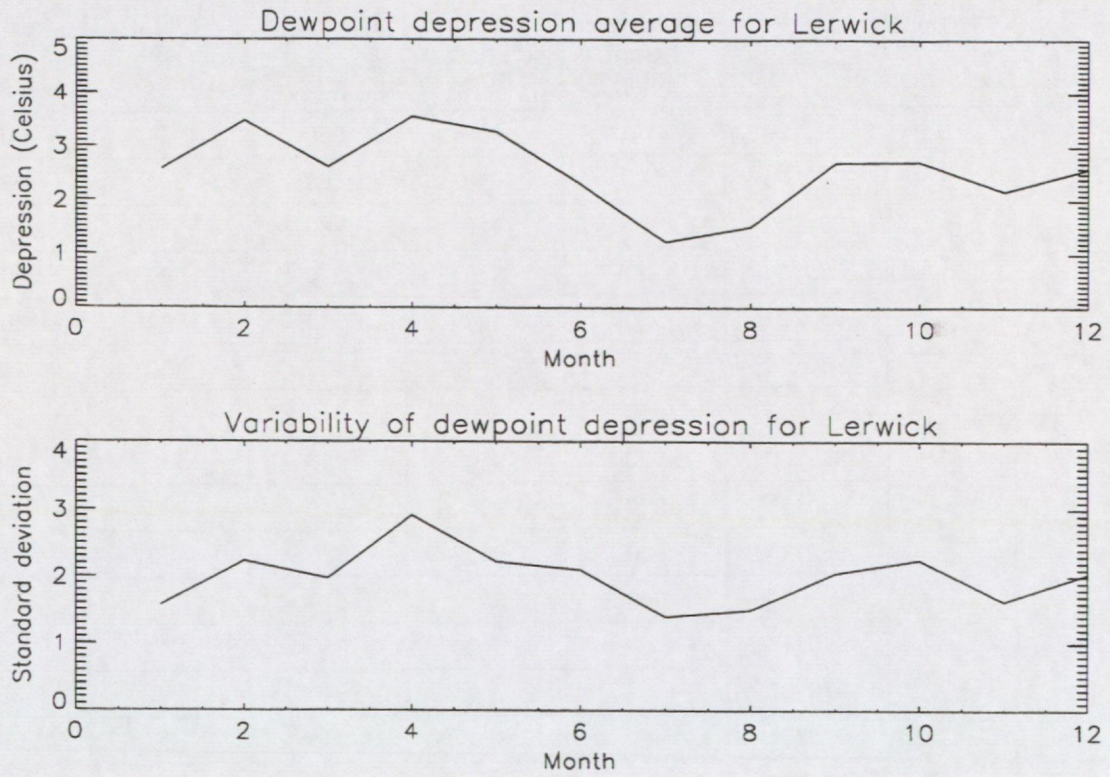


**Figure 37: Monthly mean of the dew-point depression (top graph) and monthly standard deviation of the dew-point depression (bottom graph) for Lerwick in 1997.**

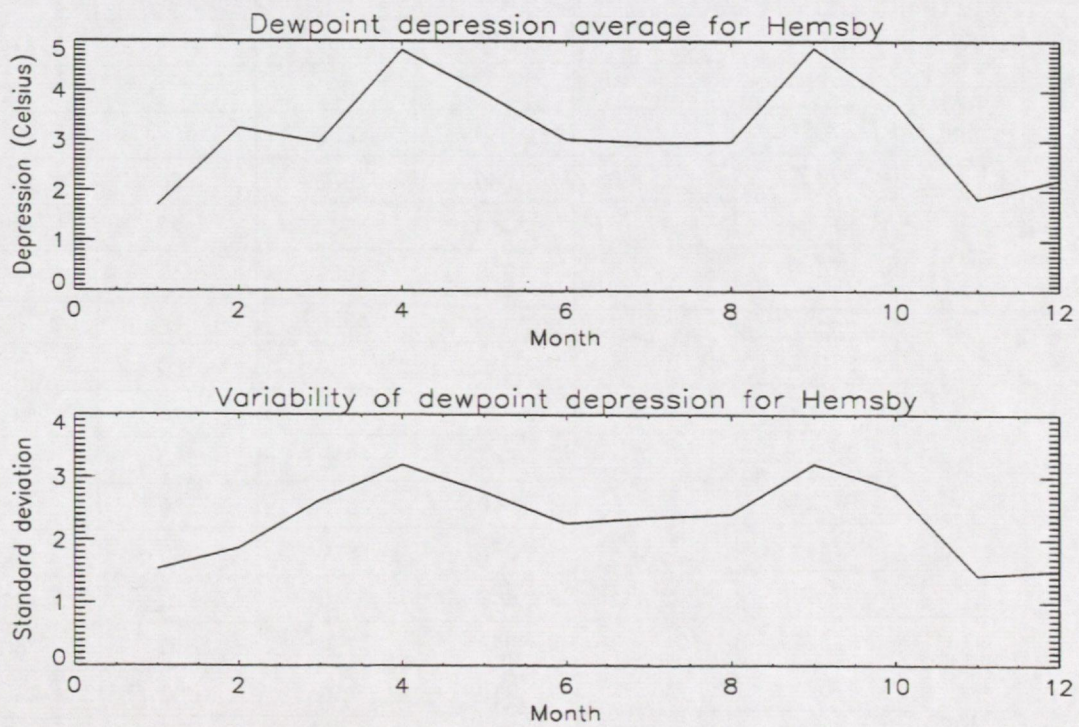


**Figure 38: Monthly mean of the dew-point depression (top graph) and monthly standard deviation of the dew-point depression (bottom graph) for Hemsby in 1997.**

	Date (yyymmdd)	Helicopter height (hPa)	Convective cloud base (hPa)	Freezing level (hPa)	Cloud depth (hPa)	Positive CAPE (J kg <sup>-1</sup> )
Strike cases	961126	950	900	950	160	40
	960208	960	940	980	340	280
	951208	950	920	960	330	140
	950301	920	940	940	560	600
	950221	930	900	940	530	360
	950119	900	930	920	450	260
	941003	960	890	940	320	140
	930220	900	950	940	380	110
	930218	930	900	910	200	80
	930115	920	900	880	460	130
	921030	940	900	930	70	3
Lerwick null cases	970118		940	880	170	20
	970202		870	940	110	30
	970204		900	940	230	150
	970207		900	940	490	290
	970211		930	920	500	340
	970218		870	910	470	260
	970220		900	930	430	170
	970221		900	950	500	240
	970224		920	890	540	170
	970303			930		0
	970326		910	850	100	10
	970327		940	900	450	250
	970328		910	930	220	150
	970403		950	960	540	640
	970405		950	950	240	90
	970421		910	960	180	140
	970424		940	920	210	80
	970506		940	920	560	570
970913		940	870	630	1000	
971113		950	870	590	190	
971130		840	940	310	110	
Hemsby null cases	970621		940	790	610	740
	970713		910	710	660	720
	970828		970	740	720	840

**Table 3: The convective cloud base, freezing level, cloud depth, CAPE, and helicopter height, all obtained from radiosonde data.**

	Convective cloud base (hPa)	Freezing level (hPa)	Cloud depth (hPa)	Positive CAPE (J kg <sup>-1</sup> )
<b>Strike</b>				
Minimum	890	880	70	3
Maximum	950	980	560	600
Mean	915	935	345	200
<b>Lerwick &amp; Hemsby null cases</b>				
Minimum	840	710	100	0
Maximum	970	960	720	1000
Mean	919	898	411	300
<b>Lerwick null cases</b>				
Minimum	840	850	100	0
Maximum	950	960	630	1000
Mean	916	919	374	230

**Table 4: Minimum, maximum and mean values of convective cloud base, freezing level and helicopter height obtained from radiosonde data**

### Radiosonde results for the strike cases

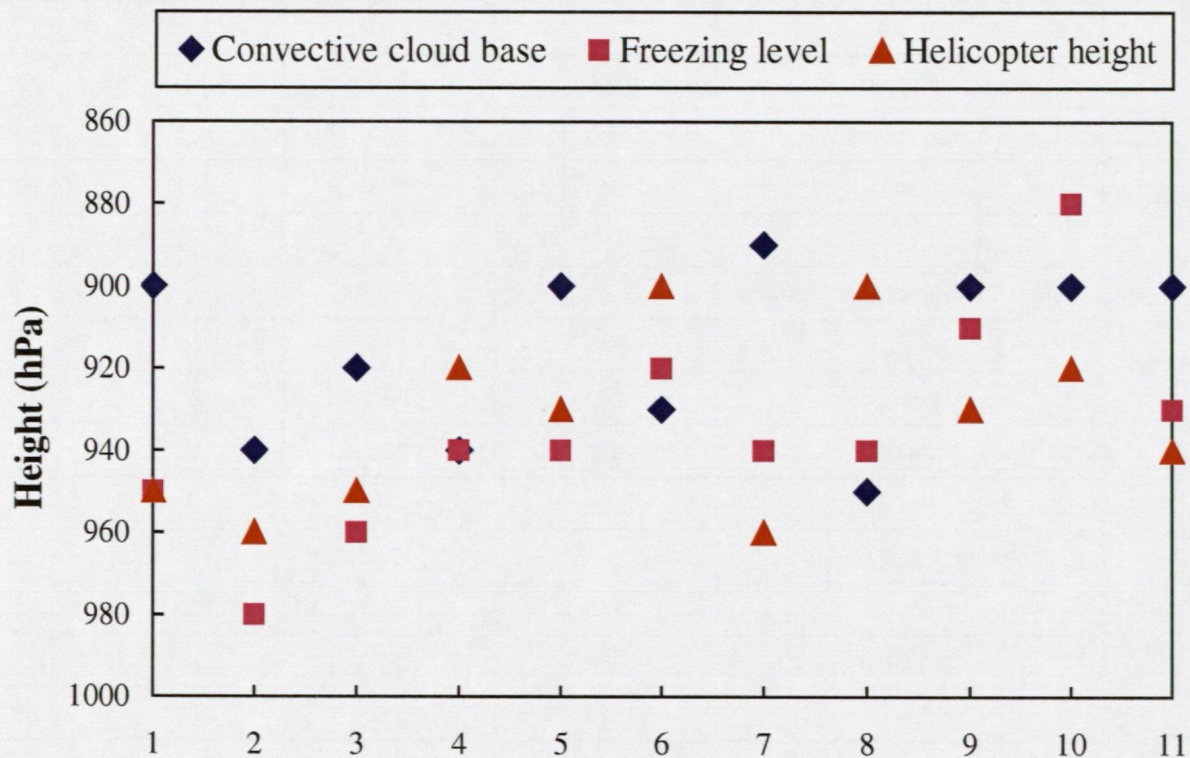


Figure 39: Relative positions of convective cloud base, freezing level and helicopter height

### Convective cloud base, freezing level and helicopter height for the strike cases

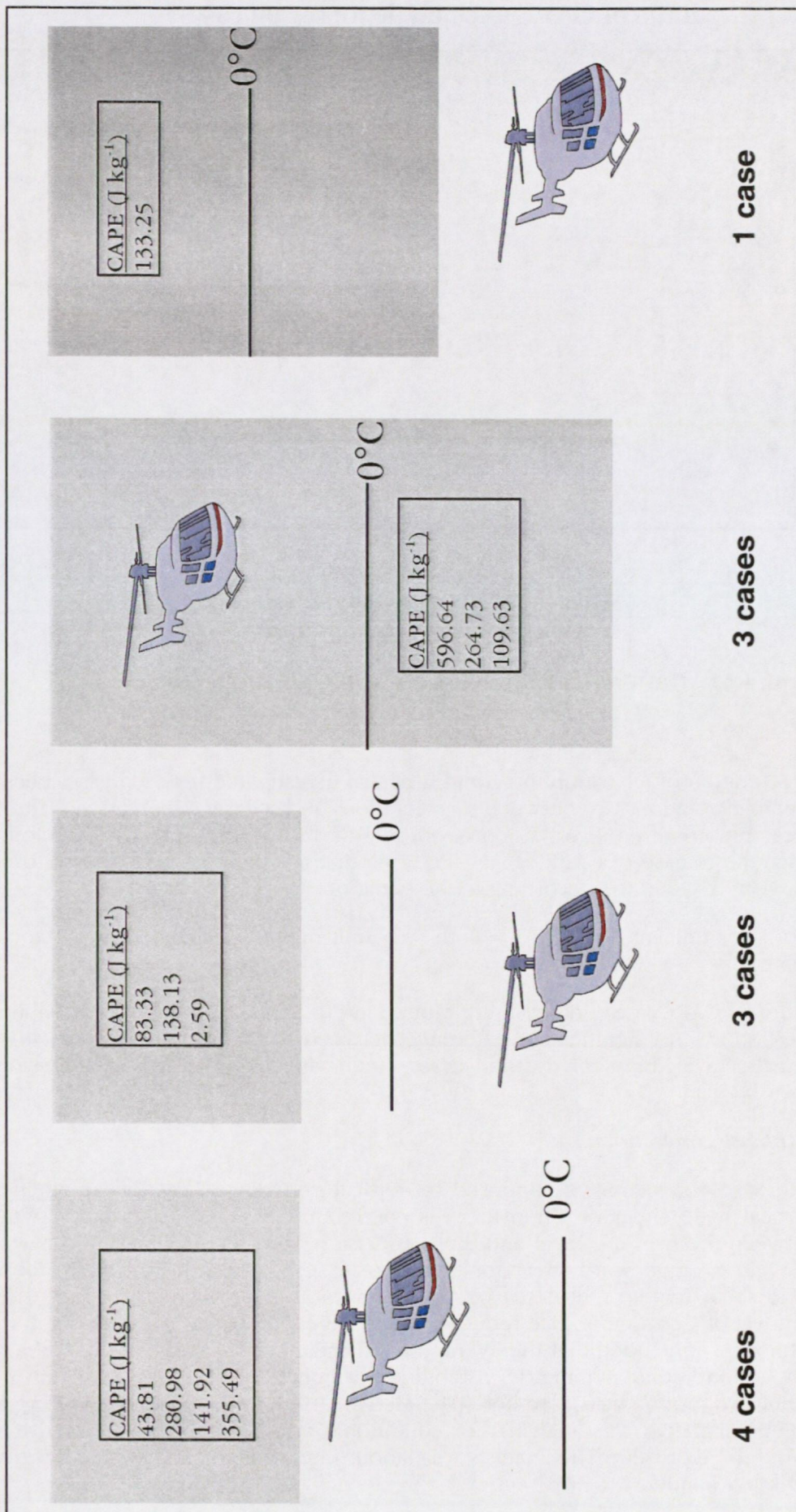
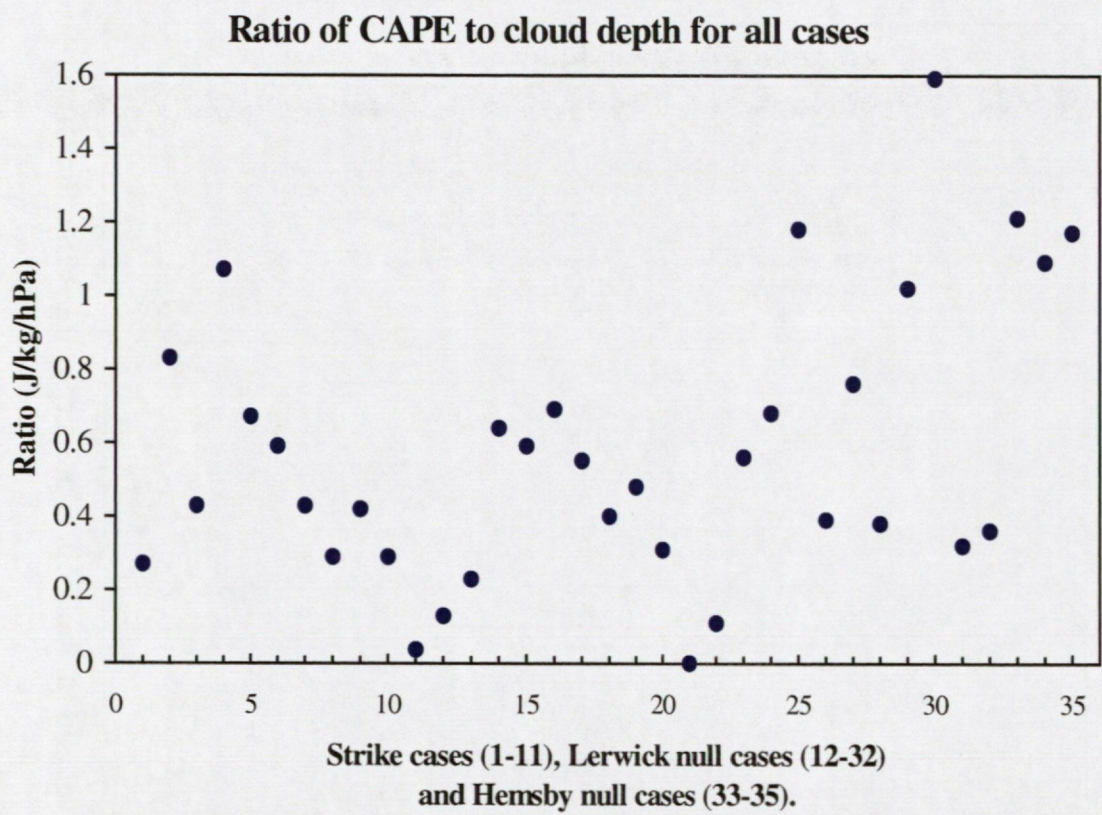


Figure 40: Altitude orderings of the convective cloud base, the freezing level and the helicopter height for the strike incidents. The CAPE values for each of the incidents are also shown



**Figure 41: CAPE/cloud depth for the strike and null cases.**

4.3.2 *Acceleration*

Acceleration of air within the cloud was also investigated for each case, because of a possible relationship between acceleration and charge separation. The vertical acceleration within a cloud is proportional to the CAPE divided by the cloud depth, since the release of CAPE causes lifting of air from the convective cloud base to the convective cloud top according to the equation

$$\text{Work per unit mass (CAPE)} = \text{Force per unit mass (Acceleration)} \times \text{Distance (Cloud depth)}.$$

Ratios of CAPE to cloud depth are plotted in Figure 41 for the strike and null cases. A t-test shows no significance difference between the mean ratio for the strike cases and the mean ratio for the null cases, both with and without the inclusion of the Hemsby data.

4.3.3 *Slantwise convection*

Slantwise convection, as opposed to vertical convection, can occur when there is vertical wind shear or when there is conditional symmetric instability. Wind shear between the freezing level and the  $-10^{\circ}\text{C}$  isotherm was examined and it was found that the average wind shear for the strike cases was 8.9 knots, while the average wind shear for the null cases was only 7.6 knots. However for the strike cases the removal of 1 particular case reduced the average wind shear to 6.4 knots. It therefore cannot be concluded that the average wind shear differs between the strike and null cases. Conditional symmetric instability is a complex instability mechanism and its details will not be discussed here (see McCann 1995). The incident that took place on 8 February 1996 was analysed for conditional symmetric instability, and it was not found to be present. The analysis was labour intensive and so it was not repeated for the other incidents.

## 5 REGRESSION ANALYSIS

Linear regression analysis was used to search for a relationship between the NWP data for a particular case and the category of that case, the category being a strike case, a Lerwick null case, or a Hemsby null case.

### 5.1 The independent variables

For each strike and null case, NWP variables considered for use in the regression analysis were taken from the model grid point closest to the incident location. Average and maximum values for particular variables were also taken from the 4 grid points surrounding the incident in the horizontal dimension.

3 different CAPE values for each case were also considered for use in the regression analysis. These were CAPE between the convective cloud base and the  $-10^{\circ}\text{C}$  isotherm, CAPE between the convective cloud base and the  $-15^{\circ}\text{C}$  isotherm, and CAPE between the convective cloud base and the convective cloud top. The square root of CAPE between the convective cloud base and an isotherm is proportional to the updraft velocity in the cloud at that isotherm, and the updraft velocity in the region between  $0^{\circ}\text{C}$  to  $-20^{\circ}\text{C}$  is particularly important for cloud electrification because this is where charge separation primarily occurs (Volland 1995, Kitagawa 1994).

The complete list of variables was

- Temperature
- Average temperature
- Relative humidity
- Vertical velocity
- Maximum vertical velocity
- Convective rain rate
- Maximum convective rain rate
- Convective cloud depth
- Cloud ice content
- Cloud water content
- Freezing level
- Positive CAPE up to the cloud top
- Positive CAPE up to the  $-10^{\circ}\text{C}$  isotherm
- Positive CAPE up to the  $-15^{\circ}\text{C}$  isotherm
- Cloud base above or below freezing level (a logical parameter).

These variables were examined for correlations of over 90%. It was found that CAPE up to the  $-10^{\circ}\text{C}$  isotherm and CAPE up to the  $-15^{\circ}\text{C}$  isotherm were highly correlated with CAPE up to the cloud top. These two variables were therefore discarded. It was also found that the freezing level was highly correlated with the temperature, so the freezing level was discarded. No other significant correlations were found.

It should be noted that

- Vertical velocity relates to the large-scale vertical motion of air, not the small-scale updraft velocity inside a convective cloud. A negative value of vertical velocity indicates ascent and therefore instability which can lead to convective cloud formation.
- Vertical velocity and relative humidity were not available on all model levels for the incidents in 1992 and 1993.
- Convective rain rate, cloud water content and cloud ice content were unavailable for the incidents in 1992 and 1993.

## 5.2 The dependent variable

The dependent variable for each case was assigned a value according to

Actual outcome = 0 for a Lerwick null case,  
1 for a strike case,  
2 for a Hemsby null case.

## 5.3 Results

The regression analysis was performed both with and without the inclusion of the Hemsby null cases, using a stepwise technique to select the variables that best distinguished between the strike and null cases. The resulting regression equations were

Regression outcome (with Hemsby null cases)

$$= -8.65 - 4490 \text{ CRR} + 0.0304 \text{ CAPE} + 0.331 \text{ T} - 3.90 \text{ VV}$$

and

Regression outcome (without Hemsby null cases)

$$= 19.1 - 0.0683 \text{ T} - 2.61 \text{ VV},$$

where CRR is convective rain rate in  $\text{kg m}^{-2} \text{ s}^{-1}$ , CAPE is convective available potential energy in  $\text{J kg}^{-1}$ , T is temperature in Kelvin, and VV is vertical velocity in  $\text{Pa s}^{-1}$ .

With the inclusion of the Hemsby null cases, CAPE and convective rain rate were probably selected to distinguish between the Lerwick and Hemsby null cases. The selection of convective rain rate means that the regression outcome cannot be calculated for the 4 oldest strike cases because of the unavailability of the convective rain rate for these cases.

With and without the inclusion of the Hemsby null cases, vertical velocity may have been selected because frontal activity was present for the strike cases but possibly absent for the null cases. It is unclear why the temperature was selected.

Further results for the regression analysis that included the Hemsby null cases are presented in Tables 5 to 7. Table 5 gives the goodness of fit of the regression

equation, Table 6 gives the coefficients for each of the selected variables and their significance, and Table 7 is a contingency table that compares the forecast outcomes with the actual outcomes. The forecast outcomes were found by rounding the outcomes given by the regression equation to a discrete value according to

Forecast outcome = 0 for regression outcome < 0.5,  
 1 for 0.5 < regression outcome < 1.5,  
 2 for regression outcome > 1.5.

Equivalent results for the regression analysis that excluded the Hemsby null cases are presented in Tables 8 to 10.

R <sup>1</sup>	R square <sup>2</sup>	Adjusted R square <sup>3</sup>	Standard deviation of the regression outcome error
0.715	0.511	0.437	0.504

**Table 5: Regression equation goodness of fit for Hemsby null cases included**

	Coefficient	Standard deviation of the coefficient error	t <sup>4</sup>	Significance <sup>5</sup>
(Constant)	-8.65	7.42	-1.17	0.254
Convective rain rate	-4490	1930	-2.32	0.0283
Total positive CAPE	0.0304	0.0088	3.44	0.0020
Temperature	0.0331	0.0270	1.23	0.231
Vertical velocity	-3.90	1.57	-2.48	0.0198

**Table 6: Regression equation coefficients for Hemsby null cases included**

<sup>1</sup> R is the correlation coefficient between the regression outcomes and the actual outcomes. It has a value between -1 and +1. The greater the absolute value of R, the better the correlation.

<sup>2</sup> R square is the square of R and therefore has a value between 0 and 1.

<sup>3</sup> Adjusted R square is the value of R square adjusted for the population rather than the sample. The adjustment takes into account the number of cases and the number of selected independent variables.

<sup>4</sup> t indicates the level of importance of the variable relative to the other variables. The higher the absolute value of t the greater the importance the variable.

<sup>5</sup> The significance is the percentage probability that the variable concerned is irrelevant. The lower the significance the more important the variable.

		Forecast		
		Strike	No strike	Total
Actual	Strike	3	4	7
	No strike	3	21	24
	Total	6	25	31

**Table 7: Contingency table for forecasts calculated using the regression equation for Hemsby null cases included.**

R	R square	Adjusted R square	Standard deviation of the regression outcome error
0.5504	0.3029	0.2548	0.4166

**Table 8: Regression equation goodness of fit for Hemsby null cases excluded.**

	Coefficient	Standard deviation of the coefficient error	t	Significance
(Constant)	19.1	8.58	2.23	0.0338
Temperature	-0.0683	0.0312	-2.19	0.0368
Vertical Velocity	-2.61	0.926	-2.81	0.0087

**Table 9: Regression equation coefficients for Hemsby null cases excluded**

		Forecast		
		Strike	No strike	Total
Actual	Strike	7	4	11
	No Strike	0	21	21
	Total	7	25	32

**Table 10: Contingency table for forecasts calculated using the regression equation for Hemsby null cases excluded**

		Forecast		
		Strike	No strike	Total
Actual	Strike	2	5	7
	No strike	5	19	24
	Total	7	24	31

		Forecast		
		Strike	No strike	Total
Actual	Strike	4	7	11
	No strike	7	14	21
	Total	11	21	32

**Tables 11 and 12: The contingency tables that would be expected for random forecasts for Hemsby null cases included (left) and Hemsby null cases excluded (right).**

Comparing Tables 5 and 8 it can be seen that the adjusted R square value is much better when the Hemsby null cases are included in the analysis. However the forecasting accuracy is significantly better when the Hemsby cases are excluded, as can be seen by comparing Tables 7 and 10. With the Hemsby null cases included in the analysis the regression equation correctly forecasts only 3 of the 7 strike cases and 21 of the 24 null cases, but when the Hemsby null cases are excluded the equation correctly forecasts 7 out of the 11 strike cases and all 21 of the null cases.

The contingency tables that would be expected for random forecasts are shown in Tables 11 and 12, for the inclusion and exclusion of the Hemsby null cases respectively. The tables were calculated by simply assuming that the probability of a strike is given by

$$\text{Probability of a strike} = \frac{\text{number of strike cases}}{\text{number of strike cases} + \text{number of null cases}}$$

$\chi^2$  tests between the contingency tables show that with the Hemsby null cases included in the analysis the probability of achieving the forecast success rate by chance alone is quite high. However with the Hemsby null cases excluded from the analysis this probability is less than 1%. Future discussion of the regression analysis results will therefore consider the Hemsby null cases excluded situation only, for which the regression outcomes are plotted in Figure 42.

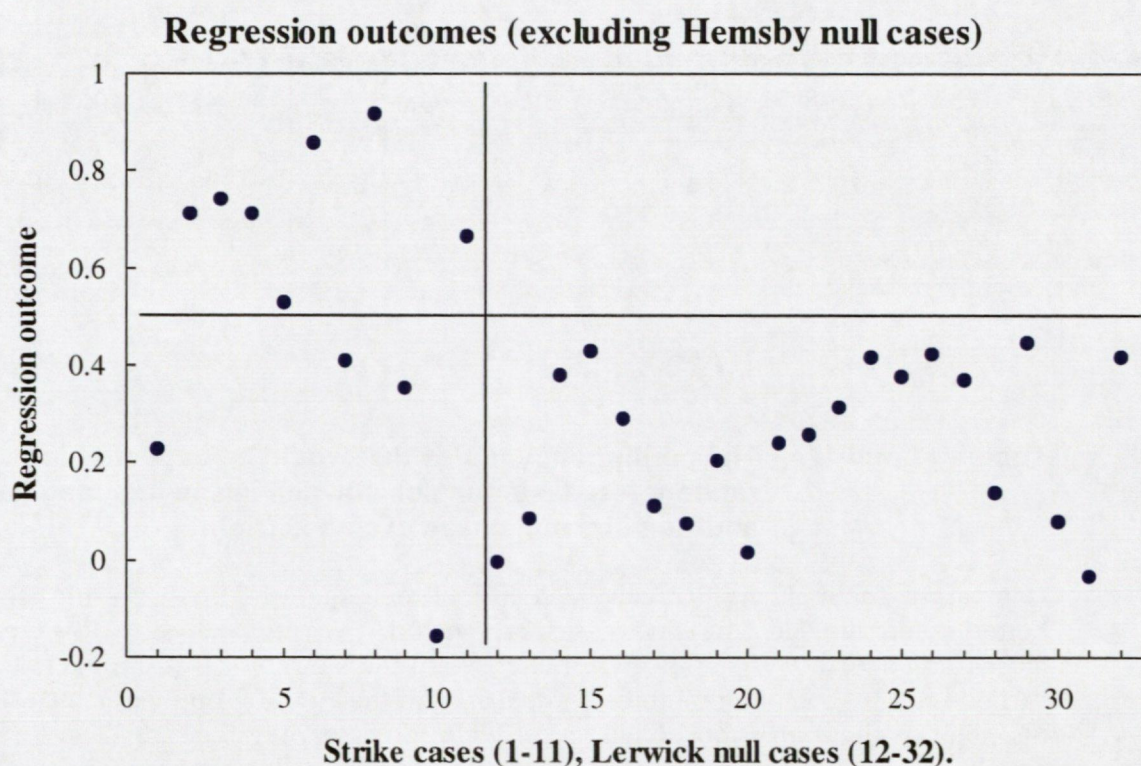


**Figure 42: Regression outcomes for the Hemsby null cases excluded**

## 6 DISCUSSION

Ascent of air on both small and large scales seems to contribute to the initiation of helicopter lightning strikes. Convective activity was observed from the ground and confirmed by satellite imagery for all 11 of the lightning strike cases investigated, and large scale vertical velocity was found to be a distinguishing feature between the strike and null cases. Large scale vertical velocity is an indicator of frontal activity, and in 10 of the 11 cases a front or trough was either present at the time of the incident or shortly before the incident

Winter thunderstorms in the North Sea are probably similar to those that occur in the Sea of Japan, since both areas have advection of dry polar air masses over warm sea currents which can lead to convective instability. The Sea of Japan thunderstorms are typically of small vertical extent, of short duration, and have low flash rates. Single flash storms are common (Kitagawa and Michimoto 1994). North Sea thunderstorms with these characteristics may be difficult to identify from a helicopter, particularly if embedded within layer cloud.

Lightning strikes to helicopters probably only occur in the presence of a strong electric field. Electric fields associated with convective clouds are caused by charge separation and the charge separation process is most efficient in high updraft velocities (Sheridan et al 1997). It is perhaps slightly surprising that CAPE was not identified in the regression analysis as being significant for distinguishing between the strike and null cases.

Lightning flash rates in the North Sea are likely to be high when cloud tops reach high altitudes, since evidence suggests that the flash rate for maritime clouds increases approximately with the square of convective cloud top height (Price and Penner 1997). However high cloud tops do not seem to be a characteristic of the helicopter lightning strikes. Although cloud top heights themselves were not examined, neither the mean convective cloud base nor the mean cloud depth differed significantly between the strike and null cases.

Flash rates may also be high when there is heavy precipitation, since Sheridan et al (1997) observed a roughly linear relationship between lightning frequency and precipitation rate. For all 11 of the lightning strike cases precipitation was observed in the region, and for 5 of the 7 strike cases for which convective rain rates were available the helicopter was on the edge of an area of high convective rain rate. However convective rain rate was not selected in the regression analysis as being significant for distinguishing between the strike and null cases.

Precipitation can also be important for aircraft charging. Flying in precipitation might cause charging of a helicopter which could in turn increase the probability of the helicopter being struck by lightning. Gardiner and Hallett (1985) found that significant charging of their aircraft occurred in cloud in the presence of ice, and in this study cloud ice was found to be in the vicinity for 4 of the 7 strike cases for which cloud ice values were available. However tephigram analyses showed that the helicopter was below the convective cloud base in 8 out of the 11 cases, so that it is unclear whether helicopter charging could have occurred.

Gardiner and Hallett also found that lightning strikes to their aircraft did not coincide with abrupt changes in the charge on their aircraft or in the local electric field, although they would not have been able to detect any horizontal field changes. Conversely Bullock and Jones (1988) found that strikes to their aircraft both discharged the aircraft and reduced the local electric field. It is thus difficult to estimate the importance of helicopter charging.

Small (1995), Hewston (1996a) and Hewston (1996b) discuss charge regions and electric fields that are not associated with convective cloud. In particular they consider a layer of dry air between 2 layers of moister air, possibly caused by the passage of a front. They suggest that precipitation falling into the dry layer could evaporate and leave behind pockets of positive charge. They also point out that dry air is less conductive than moist air so that electric fields across a dry layer could become large. For 3 of the 11 lightning strike incidents there was a layer of dryer air between 2 layers of moister air, and so perhaps these strikes were associated with dry layer electric fields.

## 7 SUMMARY

This investigation has tried to identify similarities in the meteorological conditions surrounding lightning strikes to North Sea helicopters, and has involved the detailed study of 11 lightning strike incidents.

A common feature of the incidents proved to be the presence of convective cloud, but unfortunately no obvious feature was found to distinguish between strike cases and null cases selected from days when convective cloud was present but no strike occurred. However regression analysis of NWP data for the strike and null cases produced encouraging results. A regression equation was derived that correctly forecasted 28 out of 32 strike and null cases. This equation had temperature and vertical velocity as its independent variables.

## 8 FUTURE WORK

The 4 cases for which the regression equation did not forecast a strike but a strike occurred could be re-examined in depth. Identification of the reason for these incorrect forecasts might improve our understanding of helicopter lightning strikes.

Regression equation forecasts could be verified using the 2 strike incidents that have occurred since the completion of this study, any future incidents, and the incident that took place on 26 February 1996 for which the location was identified through sferic data. The forecasts could also be verified using sferic data.

The regression equation could be updated by repeating the regression analysis with the inclusion of the additional incidents mentioned above.

There is the possibility of a SAFIR system being installed in the North Sea area. Should this become operational then additional lightning data might become available to supplement that obtained through the Met. Office lightning detection system. North Sea lightning characteristics could then be investigated. The timescale of the SAFIR project is unknown.

The regression results justify a feasibility study into the use of the regression equation for producing forecasts of lightning strike risk. Such a study should establish forecast requirements, such as when they should be issued, what altitudes they should be issued for, and whether they should be contoured according to the forecast risk level. It should also establish whether the forecasts would have a positive impact on helicopter operations, and it thus seems important that North Sea helicopter operators be involved in the study. An example of the type of forecast that could be produced is shown in Figure 43.

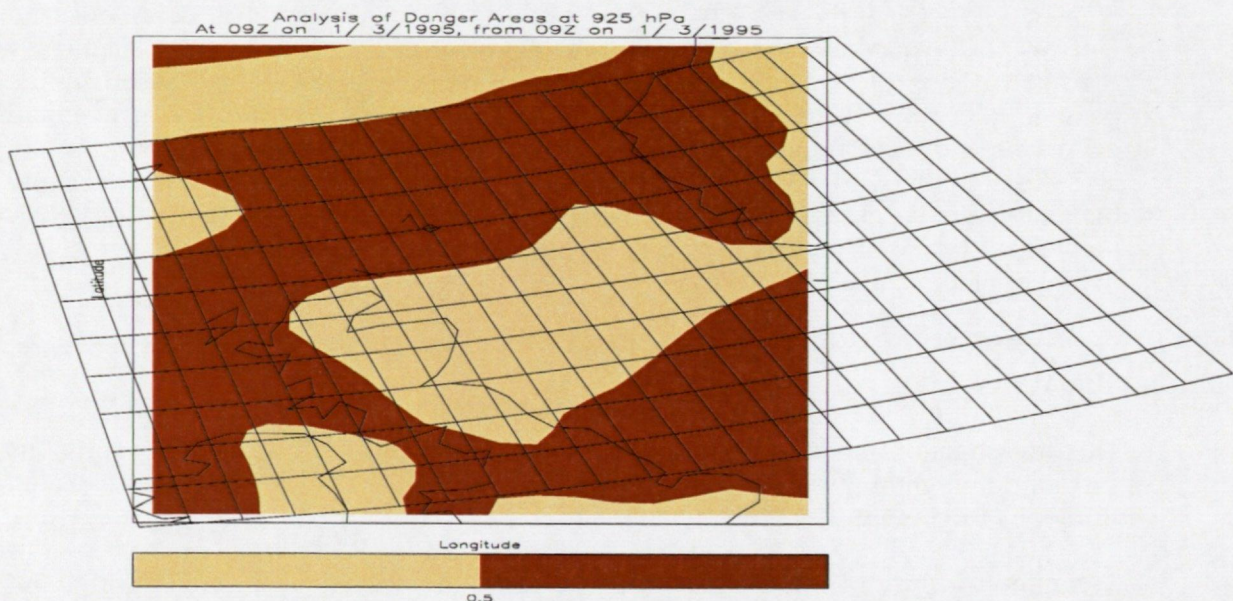


Figure 43: An example forecast of lightning strike risk

## 9 REFERENCES

- Bullock, J.W. and Jones, J.J. A chronology of in-cloud electric field and lightning strikes on an instrumented research aircraft. International aerospace and ground conference on lightning and static electricity, 1988.
- Gardiner, B. and Hallett, J., 1985: Field observations of aircraft charging in convective clouds. 10th International aerospace and ground conference on lightning and static electricity, 10–13 June 1985, Paris.
- Hewston, C., 1996a: Premature Fuzing of MPC Missiles. Internal Report, APH/7/3/95. The Met. Office, 12 March 1996.
- Hewston, C., 1996b: Premature Fuzing of MPC Missiles. Internal Report, APH/7/3/95. The Met. Office, 13 June 1996.
- Kitagawa, N. and Michimoto, K., 1994: Meteorological and electrical aspects of winter thunderclouds. *J Geophys Res*, **99**, 10,713–10,721.
- McCann, D.W., 1995: Four-dimensional computations of equivalent potential vorticity. Proceedings of the 14th Conference on Weather Analysis and Forecasting, Am Met Soc, Boston.
- Met. Office, 1994: Handbook of Aviation Meteorology. London, HMSO.
- Met. Office, 1997: The Forecasters' Reference Book. Bracknell, The Met. Office.
- Plumer, J.A., Hobbs, R., and Perala, R.A., 1996: North Sea helicopter lightning avoidance project. Produced by Lightning Technologies Inc for Bond Helicopters Ltd.
- Price, C. and Penner, J., 1997: Nox from lightning. 1. Global distribution based on lightning physics. *J Geophys Res*, **102**, D5, 5,929–5,941.
- Saunders, C.P.R., 1995: A review of thunderstorm electrification processes. *J Appl Meteorol*, **32**, 642–655.
- Sheridan, S.C., Griffiths, J.F. and Orville, R.E., 1997: Warm season cloud-to-ground lightning-precipitation relationships in the south-central United States. *Weather and Forecasting*, Vol 12, no. 3, part 1, September 1997.
- Small, R.M., 1995: Loss of towed target at Aberporth rage, 22/03/1995. Internal Report, APH/7/3/95 E13b. The Met. Office.
- Volland, H., 1995: Handbook of atmospheric electrodynamics, Volume 1. CRC Press Inc.
- Weber, M., Boldi, R., Laroche, P., Krehbiel, P. and Shao, X-M, 1993. Use of high resolution lightning detection and localization sensors for hazardous aviation weather nowcasting. Conference on Atmospheric Electricity, 4–8 October 1993, St. Louis, Missouri.

